

Relevance Is Not Permission: Warranted Attention for Value Contributions

Minwoo Yu and Young-guk Ha

Abstract—Relevance is not permission. Attention lets a model read key-value items related to the current query, but it does not ensure that the value contribution of the item is valid prediction evidence. A retrieved passage can be relevant to a question without being supporting evidence, and a historical fact or temporal neighbor can even obscure true-tail ranking or the current edge score. This paper formalizes this gap as a permission problem for the weighted value term $\alpha_{ij}v_j$ that is actually added to the prediction path. We propose Warrant, a path-localized interface that preserves attention relevance α_{ij} , exposes the value path leading to the primary metric, and, in the full model, replaces $\alpha_{ij}v_j$ with $\alpha_{ij}g_{ij}v_j$ using learned query-item permission g_{ij} . We place the same operator on metric-defining value paths for CTGD link prediction, MTPP next-mark ranking, RAG supporting evidence selection, STPP next-location forecasting, and TKG tail prediction. Across 32 paired comparisons with three seeds, for a total of 192 runs, Warrant improves the primary metric in 27 comparisons; practical tiers are 10 substantial, 1 marginal, 8 positive but uncertain, 8 tie/negligible, and 5 drops. In path-localization checks, correct-path placement exceeds direction-aware Base performance in every domain and outperforms generic attention placement by +0.1076 AUC in CTGD and +0.0683 MRR in TKG. Ablations show that most of the TKG gain comes from exposing the historical-tail value path, whereas the core CTGD gain comes from edge-conditioned query-item permission. Overall, prediction evidence is not attention mass. A weighted value term becomes evidence only when it is warranted on the path to the metric.

Index Terms—Attention weighted value term, path-localized contribution, path exposure, query-conditioned permission, evidence contribution.



1 INTRODUCTION

Attention computes relevance between a query and key-value items, then incorporates the values of highly relevant items into a prediction representation. Since the Transformer, attention has become a common computational unit beyond sequence modeling, appearing in temporal graph learning, retrieval-augmented reasoning, temporal point processes, and temporal knowledge graph forecasting [1], [2], [3], [4]. Across domains, the item read by attention may look different: a temporal neighbor, a past marked event, a retrieved passage, a spatio-temporal history element, or a historical temporal fact. In all cases, however, it is a key-value item read for the current prediction.

This work starts from the observation that attention relevance and prediction evidence are not the same concept. Attention estimates whether an item is lexically, semantically, temporally, structurally, or historically related to the current query. Prediction loss, however, requires not relevance itself but an effective contribution that supports the final prediction. In RAG, a retrieved passage can be semantically related to the question without being supporting evidence. In temporal knowledge graphs, a historical fact can be structurally connected to the current temporal query without supporting the true-tail ranking. In continuous-time dynamic graphs, a past interaction can be related to the current edge while being stale or reinforcing a hard negative. In marked temporal point processes, a past event can be useful for one candidate mark but become a shortcut

for another. Thus, a relevant key-value item is not always entitled to affect the prediction.

To address this problem, we propose Warrant. Warrant starts from the read operation produced by existing attention, retrieval, memory access, or temporal-neighbor aggregation, and explicitly models the remaining metric-facing contribution path. Specifically, it exposes the item-wise value contribution already formed by attention on the path that leads to the primary metric. In the full instantiation, it controls whether the contribution may enter the prediction-facing path through query-conditioned permission. In other words, attention decides what the model can read, whereas Warrant decides on which metric path the read value contribution is exposed and how much it should affect the current prediction. This separation is important when an item is relevant but can produce a destructive or noisy contribution, such as stale, shifted, shortcut, or ambiguous items.

Figure 1 summarizes the central distinction. Attention decides which item a query can access, whereas Warrant re-decides whether the read weighted value contribution is qualified to enter the metric-facing prediction object as evidence through path-localized permission.

The key idea of Warrant is not the mere presence of a gate, but the identification and exposure of the metric-defining value path. Changing attention scores or the retrieved candidate set mixes relevance estimation with the contribution decision again. In contrast, Warrant preserves the value contribution formed by attention and separates path exposure from learned permission on the value path leading to the primary metric. We define this placement principle as path localization. Rather than attaching a gate to an arbitrary attention layer, we find the path through

- M. Yu and Y.-g. Ha are with the Smart Computing Laboratory, Department of Computer Science & Engineering, Konkuk University, Seoul 05029, Republic of Korea. E-mail: {snowypainter, ygha}@konkuk.ac.kr.
- Y.-g. Ha is the corresponding author.

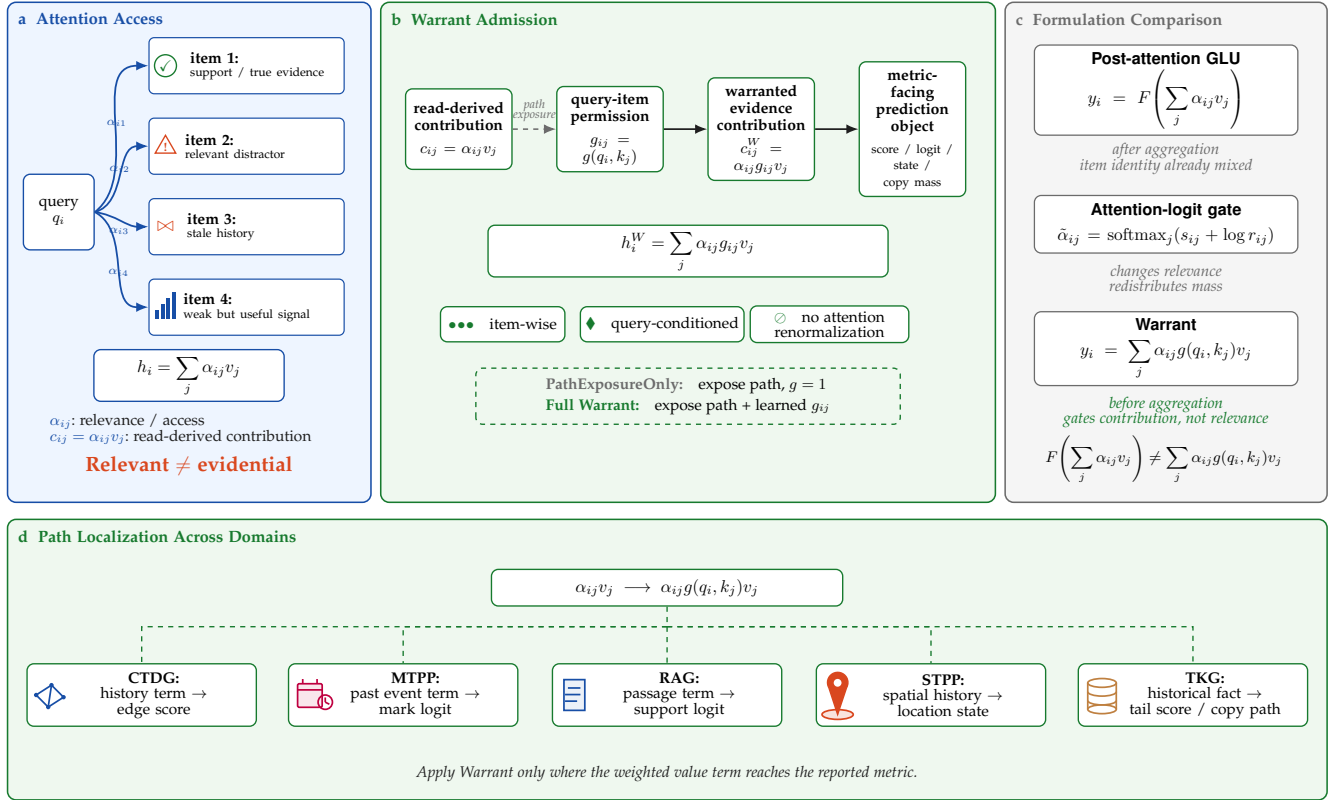


Fig. 1. Main message of Warrant. Attention gives access to relevant key-value items, while Warrant admits read-derived weighted value contributions on metric-facing paths through query-item permission. The same operation is localized across CTDG, MTPP, RAG, STPP, and TKG.

which the actual value contribution flows into the prediction object that determines the task metric, and place a value-contribution interface on that path.

Warrant also differs from generic gating, modulation, and routing in its computational target. Highway and recurrent gates control information flow through hidden states or layer transformations, FiLM modulates feature channels condition-wise, and MoE routes examples to expert paths [5], [6], [7], [8], [9]. The target controlled by Warrant is not the entire hidden state, a feature channel, or an expert path, but the prediction-facing value contribution produced item by item by attention. Therefore, the effect of Warrant must be evaluated as a specific placement of a contribution interface on a metric-defining value path, rather than as an effect of extra parameters or generic feature modulation.

We evaluate this idea in five task families: CTDG, MTPP, RAG, STPP, and TKG. The main benchmark compares each existing model as a baseline with a paired variant that adds Warrant to the same model’s metric-facing value path. The full evaluation consists of 32 paired comparisons, three seeds, and 192 completed runs; Warrant improves the primary metric in 27 of the 32 comparisons. This count is a direction-level summary rather than evidence of a uniformly strong effect, and the practical tiering separately distinguishes substantial effects, marginal effects, positive but uncertain effects, tie/negligible effects, and drops. Path-localization experiments show that placing Warrant on the value path leading to the task metric outperforms the baseline in every domain and produces much larger gains than placing it at a generic attention location, especially in CTDG

and TKG. Operator ablations, mass diagnostics, counterfactual interventions, and CTDG controls provide evidence that the improvement comes from query-item permission on the metric-facing value path, not from a simple parameter increase or attention-mass redistribution.

The contributions of this paper are as follows.

- We define the weighted value contribution produced item by item by attention as the basic computational unit of prediction evidence, and propose a path-localized value-contribution interface that separates path exposure from learned permission.
- We present a value-path adaptation methodology that separates attention relevance from evidence contribution.
- We apply the same operator to CTDG, MTPP, RAG, STPP, and TKG, and propose a path-localization procedure that identifies and targets each task’s metric-defining value path.
- Through a 192-run main benchmark, path localization, CTDG edge-query ablation, TKG operator ablation, and mass diagnostics, we report both performance improvements and evidence for how the path-localized value-contribution interface operates internally.

2 RELATED WORK

This section distinguishes Warrant from five lines of prior work. Attention and memory access select information; gating and modulation control hidden states, feature channels,

activations, or expert paths; retrieval and reranking handle candidate context before or after reading; and calibration and selective prediction adjust final confidence or rejection. Warrant targets a different computational object. After attention has already estimated relevance, Warrant decides whether the attention-weighted value contribution may affect the current prediction before the prediction is formed.

2.1 Attention and Memory Access

Bahdanau attention alleviates the fixed-length context bottleneck by allowing a decoder to softly search relevant parts of a source sentence, and the Transformer formalizes attention as a query-key-value weighted-sum operation [1], [10]. End-to-End Memory Networks apply recurrent attention over a large external memory [11]. The central question in this family is which item or memory slot the current query should read. Warrant does not choose the read target again. Instead, it separately asks whether the item-wise value contribution produced by attention or memory access may enter the prediction path.

2.2 Gating and Modulation

Gating is a general principle for controlling information flow in neural computation. Highway Networks and recurrent gates control flows through transformed inputs, carried inputs, memory-cell updates, and hidden-state updates, while GLU gates convolutional activations [5], [6], [7], [12]. FiLM applies feature-wise affine modulation from a conditioning signal, squeeze-and-excitation reweights feature channels, and MoE selects expert computation paths with a gating network [8], [9], [13]. Warrant also uses a gate. However, its gated object is an attention-derived item-wise value contribution, which is distinct from hidden states, channels, activations, and expert routes.

2.3 Gated Attention Variants

The Gated-Attention Reader builds query-specific token representations through multiplicative interactions between query and document representations; GTrXL introduces gating into Transformer architectures for training stability; and Mega combines moving averages with gated attention for long-sequence modeling [14], [15], [16]. Sparse or hard attention changes the attention support or probability distribution itself, and pointer-generator models control the mixture between generation and copy branches [17], [18], [19]. These methods improve the expressiveness, stability, or sequence-modeling capability of attention architectures. Warrant does not replace the attention architecture. It preserves the attention weight as a relevance estimate and adds a permission variable to the subsequent value contribution.

Table 1 summarizes representative gate families by their gated objects. Prior work has used gates widely inside and around attention models. The difference of Warrant lies in both the computational unit to which the gate is applied and the path on which that unit resides. Warrant does not renormalize the attention distribution; it gates the item-wise attention-weighted value term on the metric-facing value path.

2.4 Retrieval, Reranking, and Calibration

Dense retrieval fetches candidate passages, RAG and FiD integrate retrieved passages into generation, and long-context models such as Longformer enable processing of extended contexts [4], [20], [21], [22]. Passage reranking reorders retrieved candidates using query-passage scores [23]. Calibration and selective prediction adjust confidence after prediction or reject low-confidence cases [24], [25]. Retrieval and reranking mainly change the candidate set or order before or after reading, whereas calibration handles post-prediction confidence. Warrant is placed between these stages. After attention has formed a weighted contribution, Warrant computes permission before that contribution enters the metric-facing prediction path.

2.5 Positioning of Warrant

Prior work has decided what to retrieve, what to attend to, which hidden feature to modulate, which expert to route to, or how much to trust the final prediction. Warrant decides whether an already attention-weighted value contribution may affect the current prediction. Thus, the distinction of Warrant is not a redefinition of attention relevance, but a separation of relevance estimation and contribution permission into different computational decisions.

3 PROBLEM DEFINITION

Attention-based models repeat the same form of computation across many domains. A query q_i represents the current prediction request, and the model reads candidate history, retrieved context, memory items, or historical facts as key-value items (k_j, v_j) . Standard attention computes compatibility between the query and the key, then produces a softmax-normalized relevance weight.

$$\alpha_{ij} = \text{softmax}_j(s(q_i, k_j)).$$

It then gathers values into a prediction representation with a weighted sum.

$$h_i = \sum_j \alpha_{ij} v_j.$$

In this paper, a key-value item is the basic unit of attention aggregation. Depending on the domain, the item may be a temporal neighbor, a past marked event, a retrieved passage, a past spatio-temporal event, or a historical temporal fact. Table 2 summarizes each task’s key-value item and metric-defining value path.

The object whose contribution must be decided.: In standard attention, the term that item j actually adds to the prediction representation is neither the key nor the value alone, but

$$\alpha_{ij} v_j.$$

We define this term as the *weighted value term*. The attention weight α_{ij} indicates how relevant the item is to the current query, but what enters the final prediction is not scalar relevance itself; it is the value contribution multiplied by relevance. Therefore, from the perspective of prediction, the important question does not end with “which item is relevant?” A more precise question is “may the already formed weighted value term $\alpha_{ij} v_j$ enter the current prediction state or score?”

TABLE 1

Taxonomy of prior work by gated object. The distinction of Warrant lies in the combination of an item-wise weighted value term and a metric-facing value path.

Family	Gated object	Gate unit	Attention renormalized	Difference from Warrant
Highway / recurrent	layer, carry, or memory update	vector / channel	no	layer-level flow
GLU / gated FFN	hidden activation	token / channel	no	activation-level gate
SE / channel attention	feature channel	channel	no	channel-level gate
Attention-logit / sparse attention	relevance score or support	item logit / item set	yes	changes α_{ij} and redistributes mass
MoE gate	expert output mixture	expert	mixture-normalized	expert-routing gate
Copy / pointer gate	generation-copy branch	branch / candidate	branch-normalized	task branch gate
Post-attention gate	$h_i = \sum_j \alpha_{ij} v_j$	aggregate vector	no	item identity is already mixed
Warrant	$\alpha_{ij} v_j$	query-item weighted value term	no	gates metric-facing contribution directly

TABLE 2

Key-value items and metric-defining value paths by task. Warrant uses the same permission operator across domains and targets the weighted value path that reaches the primary metric.

Domain	Key-value item	Prediction target	Metric-defining value path
CTDG	temporal neighbor / interaction history	current source-destination edge	edge score
MTPP	past marked event	next event mark	candidate mark logit
RAG	retrieved passage	supporting evidence passage	support ranking logit
STPP	past spatio-temporal event	next event location	next-location dynamics state
TKG	historical temporal fact	tail entity	tail ranking score / copy path

Relevance is not permission.: Existing attention binds relevance and contribution permission into the same scalar α_{ij} . Once an item receives high relevance, its value term enters the representation through the same weight. However, the task loss requires not relevance itself but an evidence contribution that supports the current label, ranking, location, event mark, or edge score. These two notions diverge across domains.

- In RAG, a retrieved passage can be relevant because it has lexical or semantic overlap with the question, but it may not be supporting evidence for the answer.
- In temporal knowledge graphs, a historical fact can be connected to the current (*head, relation, time*) query without being evidence that raises the current true tail.
- In continuous-time dynamic graphs, a past interaction can be related to the source or destination while being stale, or while reinforcing a hard negative or outdated preference for the current edge prediction.
- In marked temporal point processes, the same past event can be transition evidence for one candidate mark but a spurious shortcut for another.
- In spatio-temporal forecasting, a nearby past location can be relevant history, but if reflected too strongly it can create local copy bias rather than next-location dynamics.

Thus, relevance explains why an item should be read, but it does not guarantee that the value of the item is entitled to affect the current prediction.

Why this problem matters.: This distinction matters because the attention output is a computational path that directly reaches the downstream metric. Once $\alpha_{ij} v_j$ enters a representation, candidate score, copy mass, support logit, or dynamics state, the term functions as prediction evidence rather than merely retrieved context. If a relevant but non-evidential item enters this path, the model can rank a

distractor passage as support, use stale temporal history as evidence for the current edge, copy a repeated historical tail as if it were the current answer, or reinforce local bias in next-location prediction. Conversely, if a valid evidence term does not pass through sufficiently, the model can find the item with attention yet fail to improve the primary metric.

Therefore, the problem is not to normalize attention better, but to decide contribution qualification on the metric-facing value path. Merely changing attention mass entangles the effect of using one item less with the effect of redistributing that mass to other items. Changing the retrieved set, memory access, temporal-neighbor sampling, or historical-fact retrieval itself also entangles relevance estimation with evidence contribution. What is needed is a separate interface that preserves the weighted value term produced by attention while deciding, conditioned on the query, whether that term may enter the current prediction-facing path.

Problem statement.: For each prediction request i and key-value item j , base attention forms a weighted value term $\alpha_{ij} v_j$. The problem addressed in this paper is the following permission decision. Given $(q_i, k_j, \alpha_{ij} v_j)$, should this weighted value term affect the current prediction? The solution is not to hand-code domain-specific rules, but to learn contribution permission between the current query and item from the task loss. The method that follows therefore keeps α_{ij} as relevance, places a separate permission variable on the weighted value term, and learns which contributions become prediction evidence on the value path leading to the primary metric.

4 METHOD

Warrant uses the item-wise attention-weighted value term produced by standard attention as its computational target.

This choice distinguishes it from methods that gate attention logits, hidden states, or post-attention aggregates.

$$c_{ij} = \alpha_{ij}v_j. \quad (1)$$

The full Warrant replaces this term before aggregation, on the value path leading to the primary metric, as follows.

$$c_{ij}^W = \alpha_{ij}g_{ij}v_j, \quad h_i^W = \sum_j c_{ij}^W. \quad (2)$$

Thus, the distinction of Warrant comes from the object and path to which the gate is applied. Attention relevance α_{ij} is not softmax-renormalized, and the empirical effect decomposes into metric-facing path exposure and learned query-item permission. This section describes the interface, theoretical properties, path localization, and domain adaptation. Figure 2 summarizes the full interface.

4.1 Path-Localized Warrant Interface

For each query-item pair, the full Warrant interface computes a scalar contribution score as in Eq. (3).

$$\psi(q_i, k_j) = w^\top \text{GELU}(W_q q_i + W_k k_j) + b. \quad (3)$$

This score is transformed into the leak-sigmoid contribution scaling variable in Eq. (4).

$$g_{ij} = \lambda + (1 - \lambda)\sigma(\psi(q_i, k_j)). \quad (4)$$

Thus $g_{ij} \in [\lambda, 1]$, where λ is a leak factor that prevents any valid key-value item from being removed by a hard zero. The default value throughout this paper is 0.05. Warranted aggregation is given by Eq. (5).

$$h_i^W = \sum_j \alpha_{ij}g_{ij}v_j. \quad (5)$$

The scalar g_{ij} is the learned-permission instantiation of the interface. For decomposition, the *PathExposureOnly* diagnostic opens the same localized path but fixes $g = 1$, isolating path exposure. In the full interface, g_{ij} is learned from the query-key pair. Through the task loss, the model adjusts its own query and key representations and forms features that allow it to infer contribution scaling for the corresponding weighted value term. No domain-specific rule is injected directly into g_{ij} . Warrant controls the post-attention term without renormalizing attention logits. This placement separates the decision to read a relevant item, the decision to expose a metric-facing path, and the decision to scale the contribution on that path; it also avoids forcing the attention mass of a down-weighted item to be redistributed as relevance to other items.

Difference from generic gates.: The mathematical distinction of Warrant comes less from the sigmoid or multiplicative gate itself than from the computational unit and index to which the gate is applied. A Highway gate [5] typically mixes layer-wise information flow between a transformed path and a carry path,

$$y = T(x) \odot H(x) + (1 - T(x)) \odot x,$$

and LSTM-style recurrent gates [6] control the memory-cell update at time t ,

$$c_t = f_t \odot c_{t-1} + i_t \odot \tilde{c}_t.$$

If a simple GLU [12] is attached after attention, the aggregate $h_i = \sum_j \alpha_{ij}v_j$ has already been formed, and the gate controls an aggregate representation or channel activation,

$$\text{GLU}(h_i) = A(h_i) \odot \sigma(B(h_i)).$$

In all three cases, the gate targets hidden dimensions, layer transformations, recurrent states, or already mixed attention outputs; it does not separate whether each item-specific $\alpha_{ij}v_j$ is prediction evidence.

In contrast, Warrant places the gate on the item-wise weighted value term before aggregation.

$$c_{ij}^W = \alpha_{ij}g_{ij}v_j, \quad h_i^W = \sum_j c_{ij}^W, \quad m_{ij}^W = \alpha_{ij}g_{ij}.$$

Thus, g_{ij} creates different permissions for different item indices j within the same query i , without softmax-renormalizing the relevance distribution defined by α_{ij} . In general, the post-attention GLU $A(h_i) \odot \sigma(B(h_i))$ is not equal to $\sum_j \alpha_{ij}g_{ij}v_j$. The former is common channel scaling after item contributions have been mixed, whereas the latter is evidence scaling for each weighted value term before mixing. Because of this distinction, Warrant can separately measure path exposure from Base to *PathExposureOnly* and learned query-item permission from *PathExposureOnly* to the full interface.

For stability, g_{ij} uses leak-sigmoid scaling rather than a hard mask. Every valid item retains at least a λ -sized contribution path, and the bias is initialized so that g_{ij} starts close to one. Training therefore starts near the base attention model and gradually lowers the contribution of specific query-item pairs only when required by the task loss.

4.2 Theoretical Properties and Optimization Scope

Warrant reparameterizes the metric-facing weighted value term $c_j = \alpha_j v_j$ with item-wise permission while preserving attention relevance α_{ij} . This operation is not equivalent to either a post-attention gate or an attention-logit gate. A post-attention gate $F(\sum_j \alpha_{ij}v_j)$ cannot distinguish different item decompositions that produce the same aggregate. Attention-logit reweighting redistributes mass to the remaining items through softmax normalization, whereas Warrant uses $m_{ij}^W = \alpha_{ij}g_{ij}$ and does not enforce $\sum_j m_{ij}^W = 1$. Appendix A.9 and Appendix A.10 summarize this difference with a constructive check.

Contribution-level permission signal.: Let the loss be $\mathcal{L}(h^W)$. The gate logit is learned from the inner product between the weighted value term and the metric-loss gradient (Appendix A.1).

$$\frac{\partial \mathcal{L}}{\partial \psi_j} = (1 - \lambda)\sigma'(\psi_j) \langle \nabla_{h^W} \mathcal{L}, c_j \rangle. \quad (6)$$

Therefore, a contribution that increases loss receives a signal under gradient descent that lowers its permission, whereas a contribution that reduces loss receives a signal that preserves its permission. If \mathcal{L} is β -smooth and only one contribution is scaled, the ideal permission that minimizes a local smoothness upper bound is as follows (Appendix A.2).

$$g_j^* = \Pi_{[\lambda, 1]} \left(1 - \frac{\langle \nabla \mathcal{L}(h), c_j \rangle}{\beta \|c_j\|^2 + \epsilon} \right). \quad (7)$$

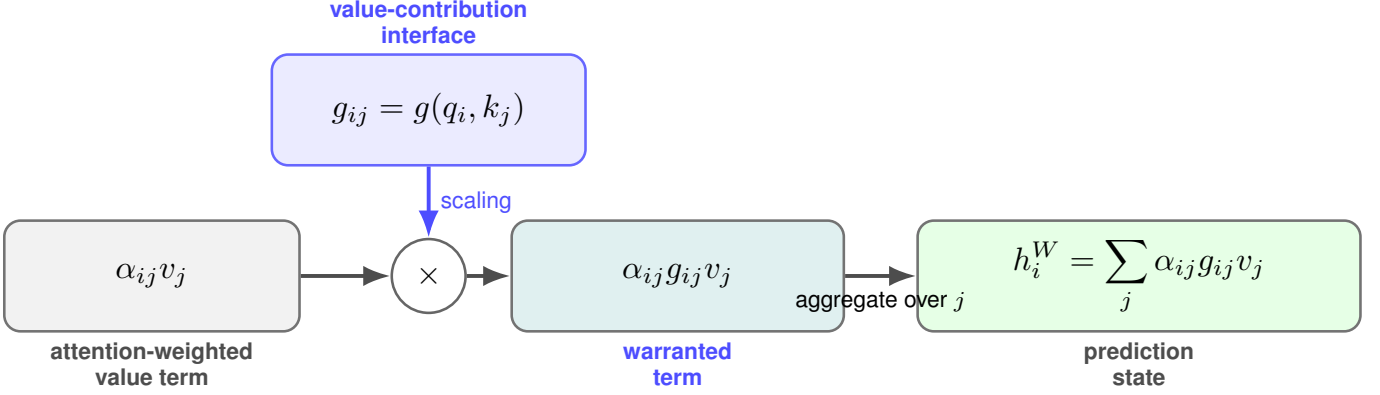


Fig. 2. Warrant interface. Attention computes item relevance α_{ij} , and Warrant exposes the post-attention weighted value term to the metric-defining path before computing the contribution scaling variable g_{ij} in the full instantiation. The prediction-facing contribution becomes $\alpha_{ij}g_{ij}v_j$.

Here, ϵ is a numerical stabilizer used when $\|c_j\|$ is small. This local rule shows why a gate that lowers harmful weighted value terms and preserves helpful weighted value terms arises naturally. The same view appears in the signal-to-noise ratio analysis. Appendix A.6 derives $\text{SNR}_W/\text{SNR}_B = R_S/R_N$, so the condition for Warrant to improve SNR is $R_S > R_N$. That is, SNR improvement depends not on perfect preservation of support contributions, but on the relative size of retained support signal versus retained noise standard deviation. Figure 3 visualizes this boundary and shows that operating points fall in the improvement region under an evidence-aligned gate regime; the simulation setting is given in Appendix B.

Manifold-local interpretation and entangled paths.:

The derivation above is written in the ambient representation space, but Appendix A.3 shows that the same rule also holds on a local representation manifold. The key is to replace ambient contributions and gradients with their tangent-space counterparts: c_j becomes $\tilde{c}_j = P_h c_j$, and $\nabla \mathcal{L}$ becomes $\text{grad}_{\mathcal{M}} \mathcal{L}$. This extension is a local descent interpretation, not a global convergence guarantee.

When multiple terms are controlled together, coupling among tangent contributions becomes important. Appendix A.4 derives the following bound for $a_j = \langle \text{grad}_{\mathcal{M}} \mathcal{L}(h), \tilde{c}_j \rangle$ and $G_{jk} = \langle \tilde{c}_j, \tilde{c}_k \rangle$.

$$\mathcal{L}(R_h(\xi(g))) \leq \mathcal{L}(h) - \delta^\top a + \frac{\beta_{\mathcal{M}}}{2} \delta^\top G \delta. \quad (8)$$

If G is nearly diagonal, item-wise Warrant is a good local shrinkage approximation. Conversely, if off-diagonal tangent overlap is large, helpful contributions and shortcut/noisy contributions can share the same local subspace, and a scalar permission variable can become conservative or miscalibrated. The synthetic simulation in Appendix C also shows that the cross term increases as tangent Gram off-diagonal mass grows and can reverse the diagonal shrinkage benefit under high curvature. This perspective is connected to the path-sensitive but entangled or saturated negative-row interpretation in Section 5.8.

Optimization scope.: The leak-sigmoid parameterization guarantees $g_j \in [\lambda, 1]$, $|\partial g_j / \partial \psi_j| \leq (1 - \lambda)/4$, and $\|\Delta(g)\| \leq (1 - \lambda) \sum_j \|c_j\|$ (Appendix A.5). Thus, Warrant is a smooth bounded perturbation of the base value path.

Under standard smooth nonconvex SGD assumptions, the Warrant-augmented model inherits the usual convergence-to-stationarity guarantee. This does not imply global convergence or guaranteed improvement over the base model. It only states that Warrant preserves smooth trainability while providing a local descent-aligned evidence-admission signal.

4.3 Path Localization

Warrant targets the metric-defining value path that leads to the primary metric. Operationally, a metric-defining path is the last item-wise bottleneck through which a key-value item's weighted value term actually changes the input to the prediction object from which the reported primary metric is computed. The mere presence of an attention block, or the fact that a hidden representation changes, is not sufficient for a path to be metric-defining.

Path localization is not black-box automatic discovery. The procedure assumes access to the model computation graph and to the tensor from which the reported primary metric is computed. Under this condition, we use the auditable tracing protocol in Algorithm 1. We expose candidate attention-derived weighted value terms, test whether perturbing each term actually changes the metric object, and then select the last item-wise bottleneck before that object. Therefore, path selection is constrained by metric-object perturbation and the item-wise bottleneck criterion rather than by arbitrary attention placement.

Algorithm 1 defines Warrant as a value-path adaptation protocol rather than a fully automatic black-box search procedure. Generic attention placement can attach an interface to an attention module, but it is not metric-defining unless perturbing its item-wise weighted value term changes the reported metric object. Table 3 summarizes the resulting implementation-level tensor paths for the evaluated domains.

4.4 Domain Adaptation

In this benchmark, CTDG, MTPP, RAG, STPP, and TKG refer to concrete prediction tasks. Therefore, Warrant adaptation focuses less on designing domain-specific auxiliary features and more on identifying the key-value aggregation path that

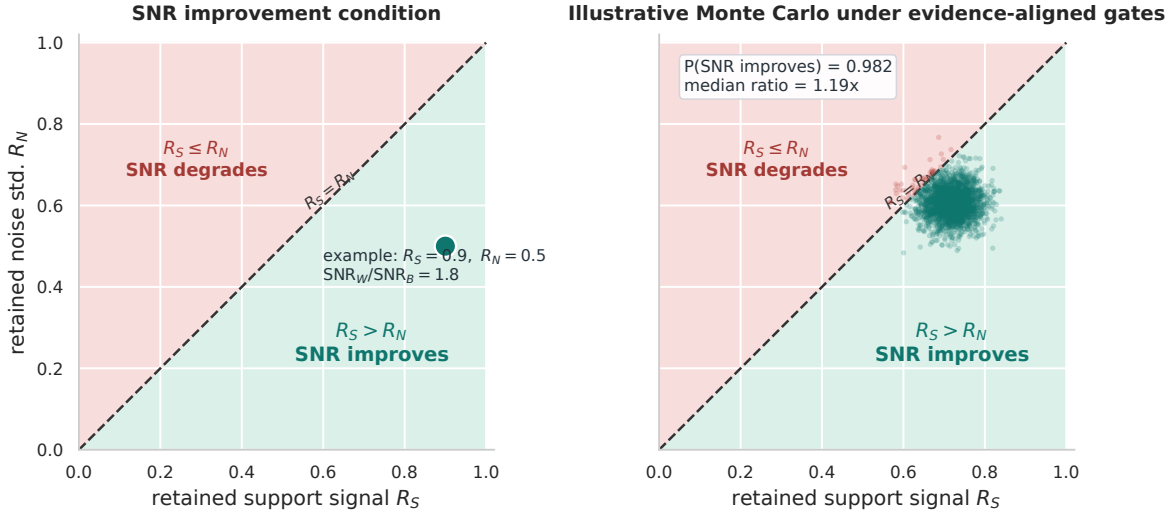


Fig. 3. SNR improvement condition under evidence-aligned permission. Left: Warrant improves SNR when retained support signal R_S exceeds retained noise standard deviation R_N . The diagonal line marks the boundary $R_S = R_N$. Right: In an evidence-aligned gate simulation, sampled operating points concentrate in the $R_S > R_N$ region.

Algorithm 1. Metric-facing value-path tracing for Warrant

Input: base model F , evaluation batch \mathcal{B} , reported primary metric m , candidate attention modules \mathcal{A} , candidate prediction objects \mathcal{Z} .

Output: metric-facing weighted value path p^* .

- 1) Identify the prediction object $z \in \mathcal{Z}$ from which m is computed, e.g., edge score, candidate mark logit, support logit, next-location state, tail score, or copy mass.
- 2) Instrument candidate attention modules. For each module, expose attention weights α_{ij} , values v_j , and weighted value terms $c_{ij} = \alpha_{ij}v_j$.
- 3) Enumerate candidate item-wise paths p . Keep only paths where $c_{ij}^{(p)}$ has an item axis j and lies upstream of z in the computation graph.
- 4) Estimate path reach by Jacobian or intervention:

$$\text{Reach}(p) = \mathbb{E}_{\mathcal{B}} \frac{\|J_{z \leftarrow c^{(p)}} c^{(p)}\|}{\|z\| + \epsilon}, \quad \text{Reach}_0(p) = \mathbb{E}_{\mathcal{B}} d(z, z[c^{(p)} \leftarrow 0]).$$

Discard paths whose perturbation changes hidden states but not the metric object z .

- 5) Select the last item-wise bottleneck before z among paths with non-negligible reach. Prefer the path closest to z that still preserves $c_{ij} = \alpha_{ij}v_j$.
- 6) Construct Warrant on p^* : $\alpha_{ij}v_j \mapsto \alpha_{ij}g(q_i, k_j)v_j$.
- 7) Validate the placement with Base vs. PathExposureOnly, Correct-path vs. Generic q-k Warrant, and Correct-path vs. Shuffled-pairing Warrant diagnostics.

TABLE 3

Summary of tensor-level path localization traced by Algorithm 1. Each row denotes the last item-wise weighted-value bottleneck whose perturbation actually changes the reported metric object.

Domain	Gated tensor	Query interface	Insertion point	Gradient path to metric
CTDG	source/destination history term	current edge query	edge-score history aggregation	AUC edge score
MTTP	past event value term	candidate mark query	candidate mark residual logit	Mark MRR candidate score
RAG	retrieved passage value term	question-passage query	support ranking logit	Support MRR passage score
STPP	spatio-temporal history term	next-event dynamics query	next-location state update	Location RMSE dynamics state
TKG	historical fact tail term	(h, r, t) query	tail score / copy path	Tail MRR ranking score

leads to each task’s primary metric and attaching the same value-contribution interface to that path.

The full Warrant interface uses the same mapping in Eq. (9) for every domain.

$$\text{Warrant: } \alpha_{ij}v_j \mapsto \alpha_{ij}g(q_i, k_j)v_j \quad (9)$$

The operator is fixed; only the weighted value path lead-

ing to the task metric and the learned query-key representations supplied by the base model to Warrant differ across domains. The application criterion is simple. The path through which the key-value item’s weighted value term is transmitted to the task metric must be exposed, and exactly that term must be used as the scaling target. We do not insert Warrant at arbitrary locations merely because

an attention layer exists. We first find the value path that determines the metric, then place the interface at the point where unchecked weighted value terms from stale, shifted, shortcut, or ambiguous items pass through that path.

CTDG link prediction.: The CTDG task is continuous-time dynamic graph link prediction, where the goal is to predict whether the current source-destination edge exists from a time-ordered interaction history. Since the prediction target is the current edge score rather than a token or node representation, the Warrant query must also represent an edge-level prediction request. Warrant constructs the current edge query through an edge-query adapter and gates source-side and destination-side temporal-history weighted terms. This adapter does not provide manual permission features such as recency thresholds, stale indicators, hard-negative labels, or overlap heuristics. It is an interface construction that exposes the model-internal representations already used by the base temporal encoder to the query-key interface of Warrant.

MTPP next-mark ranking.: The MTPP task is marked temporal point process next-mark ranking, and the primary metric is Mark MRR computed over candidate mark rankings. The same past event can act as support, a shortcut, or an ambiguous item depending on the candidate mark. If a shared sequence state scores every candidate, candidate-specific permission differences can become weak. Warrant builds a candidate query from the candidate mark embedding and the current sequence state, reads event-history values to form a candidate-specific warranted value, and provides a residual to the candidate mark logit. At this application point, Warrant asks whether a past marked event value may contribute to the current candidate mark score.

RAG supporting evidence selection.: The RAG task is formulated as retrieval-augmented supporting evidence selection. This experiment does not call an LLM or generate free-form answers; because there is no generated answer string, answer F1/EM is not evaluated. Instead, using HotpotQA sentence-level supporting facts, we define a retrieved passage that contains an annotated supporting fact as a supporting evidence passage, and use Support MRR to measure how highly that passage is ranked as the primary metric. A distractor passage can receive attention because it has lexical overlap with the question, but it is not thereby qualified to contribute to the supporting-evidence ranking score. Warrant forms warranted passage mass between the question query and retrieved passage representations and connects this mass directly to the support logit. It therefore gates the path by which weighted value terms from supporting evidence passages and distractor passages directly affect the ranking metric.

STPP next-location forecasting.: The STPP task is spatio-temporal point process next-location forecasting. The model predicts the time and continuous location of the next event, and the primary metric is Location RMSE. Unlike settings such as CTDG and TKG, where bias is added directly to a discrete candidate score, STPP determines the final metric through a continuous next-location dynamics state. Strongly copying past coordinates can create local cluster bias, and time likelihood and Location RMSE can move in different directions. Therefore, Warrant is not used

as a coordinate-copy device; it gates the path by which the prediction query reads history values to construct the next-event dynamics state.

TKG tail prediction.: The TKG task is temporal knowledge graph tail prediction. The query is (*head, relation, time*), the key-value item is a historical temporal fact, and the primary metric is tail-entity ranking MRR. A historical fact can be strong support, but a tail repeated in the past is not guaranteed to be correct for the current query. The bottleneck is therefore the path through which the historical fact value moves into the tail score or copy path. In RE-NET and xERTE, warranted mass is added to the historical tail-entity score; in CyGNet, Warrant is attached to the path on which copy mass is formed. This placement directly gates whether the tail weighted term of a historical fact may contribute to the current tail ranking.

Diagnostic criteria.: Correct adaptation should be evaluated with both performance numbers and internal signals. The difference between attention mass and warranted mass shows whether relevance and permission are separated, and candidate-wise gate differences show whether the same history is permitted differently across candidates. Support/distractor mass checks whether distractor contributions are suppressed in RAG, while stale history terms check whether old items in CTDG, TKG, and MTPP avoid excessively raising scores. In STPP and MTPP, we also examine residual scale to verify that Warrant does not overly perturb the base dynamics.

5 EXPERIMENTS

This section evaluates Warrant along several experimental axes. We first use a cross-domain main benchmark to test whether primary-metric improvements recur across task families. We then separate path exposure from learned permission through an operator ablation, and use mass and counterfactual diagnostics to show that a relevant item is not always prediction evidence. Next, a HotpotQA/RoBERTa candidate-marker control examines the effect of the gated object and path. Finally, path localization and the CTDG edge-query adapter ablation validate the interpretation of Warrant as an adaptation method for metric-facing value paths, and the Warrant Need Score (WNS) with a negative-row audit analyzes heterogeneity and drop rows.

5.1 Main Benchmark Settings

Every comparison uses the same reference implementation, seed set, and dataset/model grid, changing only the Base model versus the Warrant variant. Table 4 summarizes the training, Warrant, and model settings used in the reported benchmark.

5.2 Main Benchmark: Cross-Domain Performance

The main benchmark covers five task families: CTDG, MTPP, RAG, STPP, and TKG. We conduct 32 paired Base-versus-Warrant comparisons, and each comparison is reported as the mean and standard deviation over three seeds. The total number of completed runs is 192. Table 5 reports the paired results. Each row compares Base and Warrant for the same domain, dataset, and model, and improvement is

TABLE 4

Main benchmark settings. The benchmark runs Base and Warrant variants with the same reference implementation, seed set, and model grid.

Group	Setting	Value
Experiment	seeds	7, 17, 37
Training	epochs / max examples	30; 65,536
Training	optimizer	learning rate 0.001; weight decay 0.0
Training	history / evaluation	history length 50; evaluation ratio 0.2
Warrant	context / auxiliary loss	no context schema or fields; auxiliary weight 0.0
Warrant	gate initialization / leak	gate init 0.95; gate leak 0.05
Warrant	domain loss weights	STPP gate loss 0.0; TKG gate loss 0.0
Warrant	RAG exception	FiD/LED use gate leak 0.7 and support loss weight 1.0
Models	CTDG	Wikipedia, MOOC, LastFM with TGAT, DyGFormer, GraphMixer
Models	MTPP	StackOverflow, Retweets with SAHP, THP, AttNHP
Models	STPP	Earthquake, Gowalla with Transformer-STPP, NSTPP, DeepSTPP
Models	TKG	ICEWS14, ICEWS18, GDELTA with RE-NET, xERTE, CyGNet
Models	RAG	HotpotQA with FiD, LED

computed with the metric direction taken into account. The \pm values in Table 5 are seed-wise standard deviations; they are not row-level 95% confidence intervals or paired t -tests. Row-level paired CIs and p -values should be interpreted only when seed-wise paired deltas are reported, so the main text claims only aggregate directionality and practical tiers.

The main benchmark directly shows cross-domain performance improvements. Warrant improves the primary metric in 27 of the 32 comparisons, and the gains are not isolated to a single domain or architecture. An exact two-sided sign test provides aggregate evidence that 27/32 positive directions exceed chance-level symmetry ($p = 0.000113$). This value does not imply individual row significance, nor does it imply that every positive comparison has the same effect size. Under practical tiering, 10 comparisons are substantial, 1 is marginal, 8 are positive but uncertain, 8 are tie/negligible, and 5 are drops. In CTDG, AUC increases in all 9 combinations, and in TKG, MRR increases in 8 of 9 combinations. In STPP, Location RMSE decreases in 5 of 6 combinations, and in RAG, Support MRR increases for both HotpotQA supporting evidence selection readers. MTPP improves on Retweets but is mixed on StackOverflow.

When the value path through which attention-formed weighted value terms reach the primary metric is found and Warrant is placed on that path, direction-aware improvements recur across task families. The mean domain-level improvements are +0.0261 AUC for CTDG, +0.0002 Mark MRR for MTPP, +0.0010 Support MRR for RAG, a +0.0290 reduction in Location RMSE for STPP, and +0.0062 MRR for TKG, with an overall mean of +0.0146. These results are consistent with the interpretation of Warrant as an adaptation operator for metric-defining value paths.

Drop rows are revisited in Section 5.8 through Warrant Need Score (WNS) component decomposition and row-level failure diagnostics. The key point is that WNS is not a guaranteed performance-improvement score, but a diagnostic of path leverage or sensitivity. A row can be highly sensitive to the path, yet have zero positive PathReach and a negative main-row delta if the opened path is entangled with the

dynamics or already saturated by a useful prior path.

5.3 Separating Path Exposure from Learned Permission

In standard attention, relevance and contribution are tied to the same scalar α_{ij} .

$$\text{relevance}(q_i, k_j) \Rightarrow \alpha_{ij}, \quad \text{contribution}(j) = \alpha_{ij}v_j.$$

Changing an attention weight changes the item relevance distribution itself. In contrast, Warrant does not redefine the attention distribution; it places a separate contribution scaling variable on the weighted value term produced by attention.

$$\text{contribution}(j) = \alpha_{ij}g_{ij}v_j.$$

Thus, α_{ij} denotes key-value item relevance, g_{ij} denotes weighted-value-term permission, and $\alpha_{ij}g_{ij}v_j$ denotes the warranted contribution entering prediction-facing aggregation.

The TKG operator ablation demonstrates this separation at the level of the computational path. Table 6 reports GDELTA-xERTE variant results. This path-localization setting uses a controlled diagnostic configuration separate from the full main-benchmark configuration in Table 5. Therefore, the absolute MRR values differ from the main benchmark, and the comparison is between path exposure and learned permission under the same conditions. *PathExposureOnly* is a diagnostic that connects the historical-tail weighted value term to the metric-facing tail score while fixing every item-wise scaling variable to $g = 1$. Base \rightarrow PathExposureOnly measures the effect of exposing a missing contribution path to the score, and PathExposureOnly \rightarrow Full measures the refinement added by learned query-item permission on the opened path.

On GDELTA-xERTE, moving from Base to PathExposureOnly increases MRR by +0.0677. Moving from PathExposureOnly to the Full value gate adds +0.0010 MRR, and the Shuffled gate, which breaks the pairing between the

TABLE 5

Full main benchmark results by domain. Each row compares Base and Warrant on the same dataset and model, reporting the mean and standard deviation over three seeds. Paired Δ is the direction-aware mean difference. The \pm values are seed-wise standard deviations, not row-level 95% CIs or paired t -tests. Tier indicates the practical interpretation.

Dataset	Model	Metric	Base	Warrant	Paired Δ	Relative	Tier
CTDG			<i>continuous-time dynamic graph link prediction, AUC \uparrow</i>				
LastFM	DyGFormer	AUC	0.8482 \pm 0.0045	0.9023 \pm 0.0022	+0.0541	+6.38%	substantial
LastFM	GraphMixer	AUC	0.8806 \pm 0.0031	0.9139 \pm 0.0009	+0.0334	+3.79%	substantial
LastFM	TGAT	AUC	0.8598 \pm 0.0044	0.8897 \pm 0.0024	+0.0298	+3.47%	substantial
MOOC	TGAT	AUC	0.9639 \pm 0.0019	0.9715 \pm 0.0007	+0.0076	+0.79%	positive uncertain
MOOC	DyGFormer	AUC	0.9763 \pm 0.0003	0.9773 \pm 0.0016	+0.0010	+0.11%	tie/negligible
MOOC	GraphMixer	AUC	0.9770 \pm 0.0000	0.9774 \pm 0.0015	+0.0004	+0.04%	tie/negligible
Wikipedia	DyGFormer	AUC	0.9440 \pm 0.0015	0.9836 \pm 0.0005	+0.0396	+4.20%	substantial
Wikipedia	TGAT	AUC	0.9437 \pm 0.0027	0.9824 \pm 0.0010	+0.0387	+4.10%	substantial
Wikipedia	GraphMixer	AUC	0.9529 \pm 0.0040	0.9832 \pm 0.0003	+0.0303	+3.18%	substantial
MTPP			<i>marked temporal point process next-mark ranking, Mark MRR \uparrow</i>				
Retweets	AttNHP	Mark MRR	0.7574 \pm 0.0130	0.7653 \pm 0.0049	+0.0079	+1.06%	positive uncertain
Retweets	SAHP	Mark MRR	0.7541 \pm 0.0092	0.7578 \pm 0.0106	+0.0037	+0.49%	positive uncertain
Retweets	THP	Mark MRR	0.7584 \pm 0.0029	0.7497 \pm 0.0115	-0.0086	-1.14%	drop
StackOverflow	THP	Mark MRR	0.6066 \pm 0.0017	0.6076 \pm 0.0013	+0.0009	+0.15%	tie/negligible
StackOverflow	AttNHP	Mark MRR	0.6051 \pm 0.0020	0.6041 \pm 0.0045	-0.0010	-0.17%	drop
StackOverflow	SAHP	Mark MRR	0.6076 \pm 0.0017	0.6062 \pm 0.0017	-0.0013	-0.22%	drop
RAG			<i>retrieval-augmented supporting evidence selection, Support MRR \uparrow</i>				
HotpotQA	FiD	Support MRR	0.6555 \pm 0.0017	0.6574 \pm 0.0030	+0.0019	+0.29%	positive uncertain
HotpotQA	LED	Support MRR	0.6669 \pm 0.0018	0.6670 \pm 0.0002	+0.0002	+0.02%	tie/negligible
STPP			<i>spatio-temporal point process next-location forecasting, Location RMSE \downarrow</i>				
Earthquake	DeepSTPP	Location RMSE	1.1383 \pm 0.0288	1.0502 \pm 0.0926	+0.0881	+7.72%	substantial
Earthquake	NSTPP	Location RMSE	1.1589 \pm 0.0612	1.1159 \pm 0.1006	+0.0430	+3.84%	substantial
Earthquake	Transformer-STPP	Location RMSE	1.1147 \pm 0.0893	1.0748 \pm 0.0948	+0.0399	+3.56%	substantial
Gowalla	Transformer-STPP	Location RMSE	0.0483 \pm 0.0047	0.0460 \pm 0.0024	+0.0023	+4.38%	positive uncertain
Gowalla	NSTPP	Location RMSE	0.0486 \pm 0.0033	0.0474 \pm 0.0017	+0.0012	+2.26%	tie/negligible
Gowalla	DeepSTPP	Location RMSE	0.0481 \pm 0.0012	0.0484 \pm 0.0046	-0.0002	-0.42%	drop
TKG			<i>temporal knowledge graph tail prediction, MRR \uparrow</i>				
GDELT	xERTE	MRR	0.1277 \pm 0.0022	0.1429 \pm 0.0008	+0.0151	+11.85%	substantial
GDELT	RE-NET	MRR	0.1280 \pm 0.0011	0.1395 \pm 0.0010	+0.0115	+9.01%	marginal
GDELT	CyGNet	MRR	0.1478 \pm 0.0006	0.1478 \pm 0.0012	+0.0000	+0.02%	tie/negligible
ICEWS14	xERTE	MRR	0.2096 \pm 0.0024	0.2176 \pm 0.0032	+0.0080	+3.81%	positive uncertain
ICEWS14	RE-NET	MRR	0.2076 \pm 0.0008	0.2127 \pm 0.0046	+0.0052	+2.50%	positive uncertain
ICEWS14	CyGNet	MRR	0.2195 \pm 0.0039	0.2196 \pm 0.0031	+0.0000	+0.02%	tie/negligible
ICEWS18	RE-NET	MRR	0.1423 \pm 0.0002	0.1550 \pm 0.0025	+0.0127	+8.95%	positive uncertain
ICEWS18	xERTE	MRR	0.1515 \pm 0.0017	0.1580 \pm 0.0022	+0.0065	+4.31%	tie/negligible
ICEWS18	CyGNet	MRR	0.1536 \pm 0.0007	0.1501 \pm 0.0054	-0.0035	-2.24%	drop

TABLE 6

Controlled TKG path-exposure diagnostic on GDELT-xERTE. PathExposureOnly opens the historical-tail contribution path but fixes item-wise scaling to $g = 1$, removing learned permission.

Variant	MRR	Delta MRR vs Base	Full-Variant MRR	Interpretation
Base	0.0488	0.0000	+0.0687	no localized tail contribution path
Generic q-k gate	0.0492	+0.0004	+0.0683	generic attention placement
PathExposureOnly, $g = 1$	0.1165	+0.0677	+0.0010	path exposure without learned permission
Shuffled gate	0.1144	+0.0655	+0.0032	path exposure with broken query-item pairing
Full value gate	0.1175	+0.0687	0.0000	path exposure plus learned permission

query and fact-tail item, is 0.0032 below Full. Most of the improvement arises when the historical-tail contribution path directly enters the tail score; learned permission then provides a finer adjustment of fact-tail terms to the current query within the opened path.

This pattern matches the structure of TKG tail pre-

diction. Event sequences in GDELT and ICEWS often repeat the same entities, relation patterns, and tail entities across timestamps. Since the tail-ranking metric is determined by candidate-entity scores, recurrence signals become strong when the tail value inside a historical fact is transmitted to the current candidate score. Under conditions

where representation-only paths do not transmit this signal sufficiently to the score, simply opening the historical-tail path can yield a large gain. Learned permission then organizes this recurrence prior according to the current (*head, relation, time*) query. The TKG result therefore provides evidence for which metric path the path-localized interface should open.

5.4 Evidence Mass and Counterfactual Diagnostics

Permission is needed because a relevant key-value item is not identical to prediction evidence. In retrieval, a passage with high lexical overlap with the question can receive attention without being supporting evidence. In TKG, a historical fact can be temporally and structurally connected to the query without being true-tail evidence for the current tail ranking. In CTDG, temporal history can be related to the current edge while counterpart evidence and surrounding context differ in contribution strength. Therefore, Warrant focuses on deciding whether the weighted value term produced by attention is qualified to enter the evidence path of the current prediction.

To examine this, neural dissection is run as a restricted diagnostic experiment separate from the full main benchmark. For each domain, we select one dataset/model, use seed 7, train for 10 epochs, and record gate regimes, warranted mass, and contribution paths on at most 8192 examples. This setting is intended to test whether attention mass and warranted mass separate, and whether the localized contribution path has a counterfactual dependency on labeled evidence.

Figure 4 summarizes the relevant observations. In RAG, support attention share changes little, but warranted support mass increases and distractor mass decreases. This shows that question-passage relevance and supporting-evidence permission are not the same variable. The TKG panel shows learned gate strength together with path exposure. Even when the gate remains nearly identity in the dissection run, the localized interface can greatly improve tail ranking by opening the historical-tail contribution path. Thus, a high gate mean does not imply learning failure, and a low gate mean is not automatically better. The decisive factor is whether the contribution interface is placed on the metric-defining value path.

Table 7 reports the corresponding intervention values.

In RAG, removing supporting passage mass lowers Support MRR by 0.0030. Conversely, removing non-evidence mass raises Support MRR by 0.0034 in the oracle counterfactual. In TKG, removing true-tail evidence mass lowers MRR by 0.1162, and removing non-evidence mass raises MRR by 0.2245 in the oracle counterfactual. In CTDG, removing counterpart history mass lowers AUC by 0.0575, and removing non-evidence mass also lowers AUC by 0.0203. This indicates that surrounding temporal context in CTDG is also useful for edge prediction, while the larger dependency lies on the counterpart evidence path. Thus, permission is closer to current-query-dependent contribution scaling than to binary evidence/non-evidence masking.

RAG case study.: Figure 5 is a HotpotQA case study that visualizes raw attention, Warrant permission, and effective mass side by side on a passage-query grid. Raw

attention α_{ij} can assign mass to both supporting passages and distractor passages. Permission g_{ij} in the middle panel remains high on annotated supporting-passage cells and becomes lower on distractor cells that received attention because of lexical or contextual relevance. The effective mass $\alpha_{ij}g_{ij}$ in the right panel combines the two signals: supporting cells remain in the prediction-facing support score, while distractor cells contribute less even when they receive similar raw attention. This example shows that the attention map is not the evidence map in RAG, and that the mass entering supporting-evidence ranking is re-formed through permission.

5.5 Pretrained Transformer Encoder: HotpotQA Sentence Evidence Selection

The preceding RAG diagnostic showed that attention mass and warranted mass separate for retrieval-style passage evidence. This section moves the same question into the candidate-marker readout path of a pretrained Transformer encoder, testing whether the effect of Warrant can be explained by simply adding a gate, adding parameters, applying a post-attention gate, using an attention readout, or exposing a path. The main text summarizes the result with one control table, and Appendix E provides detailed settings and diagnostics.

The experiment fine-tunes `roberta-base` [26] for HotpotQA supporting sentence selection. Each input consists of a question, an instruction, up to 8 candidate evidence sentences, and candidate markers. The candidate set includes annotated supporting sentences, hard distractors, and random distractors, and the primary metric is Support MRR. `openpath_nogate` opens the same metric-facing candidate-marker value path while fixing $g = 1$, and `full_warrant` replaces the item-wise term $\alpha_{ij}v_j$ on that path with $\alpha_{ij}g_{ij}v_j$. The full setup and permission diagnostics are provided in Appendix E.

Table 8 shows that Warrant is not explained by parameter count or aggregate-level gating alone. `full_warrant` is +0.0098 MRR above `param_mlp`, +0.0083 MRR above `post_attention_glu`, and +0.0088 MRR above `shuffled_warrant`, which breaks query-item pairing. At the same time, `openpath_nogate` is strong, so in the HotpotQA/ROBERTa setting, opening the metric-facing candidate-marker value path itself explains an important part of the result. On top of this path, `full_warrant` adds a small learned-permission refinement and obtains the best values for MRR, R@1, Evidence F1, and Unsupported@GoldCount. AUPRC is lower than `base`. Therefore, the interpretation of this control focuses on improvements in the ranking top end and unsupported evidence attribution rather than uniform improvement across all metrics.

Unsupported evidence attribution.: Unsupported@GoldCount measures the fraction of unsupported candidates included when selecting as many evidence sentences as the number of gold supports. In the controlled candidate-evidence setting, this metric captures an evidence-attribution failure in which an unsupported sentence is selected as if it were supporting evidence; such failures can lead to downstream answer hallucination. `full_warrant` lowers Unsupported@GoldCount from

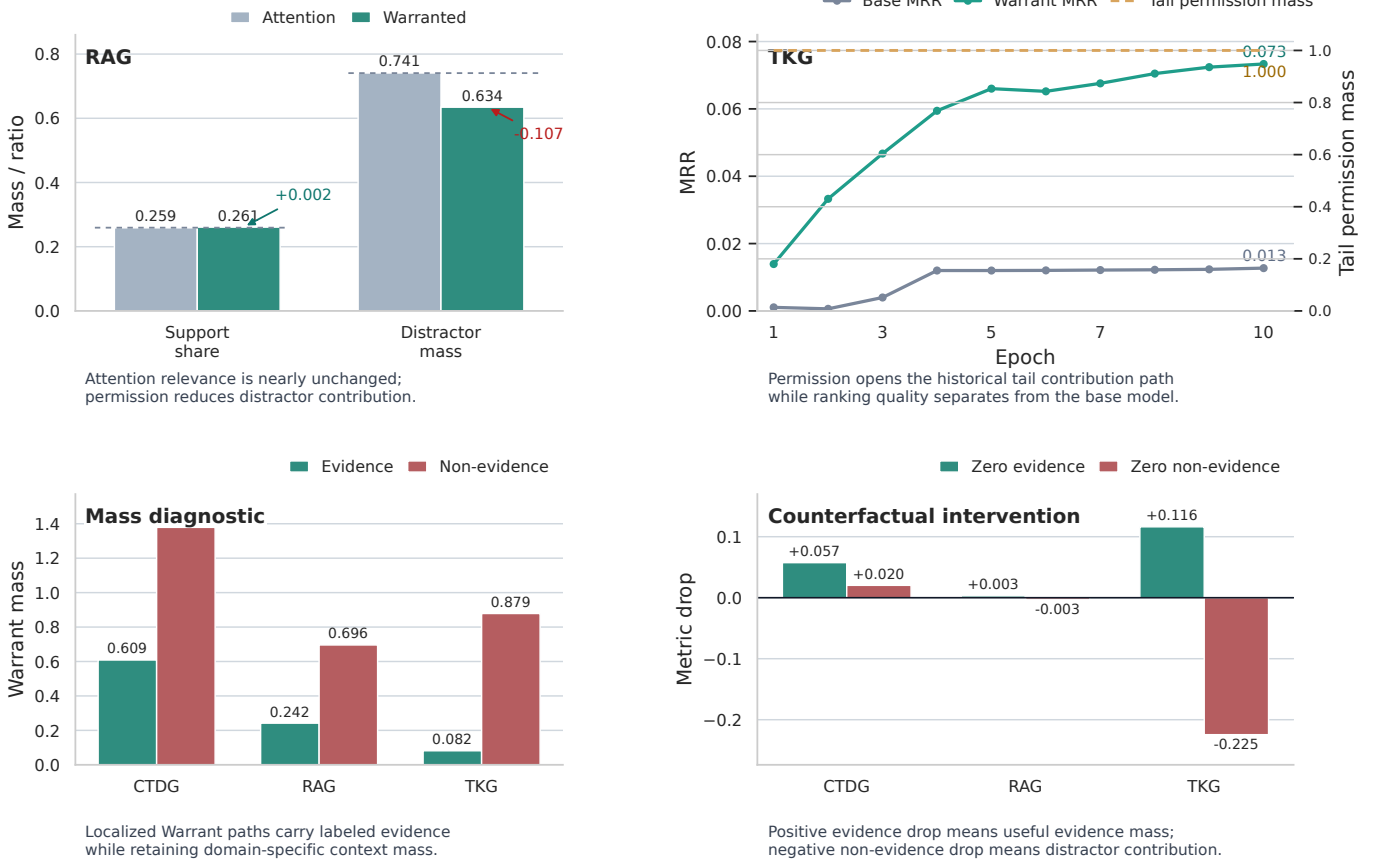


Fig. 4. Mass separation and counterfactual mass diagnostic. The upper panels show RAG relevance-permission separation and TKG path exposure, and the lower panels show CTDG/RAG/TKG zeroing interventions.

TABLE 7

Mass diagnostic using evaluation-time counterfactual interventions. A positive zero-evidence drop means that evidence mass is useful, and a negative zero-non-evidence drop means that non-evidence contribution harms the oracle counterfactual.

Domain	Metric	Primary	Evidence mass	Non-evidence mass	Drop: zero evidence	Drop: zero non-evidence
CTDG	AUC	0.8916 ± 0.0073	0.6086 ± 0.0234	1.3791 ± 0.0236	$+0.0575 \pm 0.0068$	$+0.0203 \pm 0.0012$
RAG	Support MRR	0.5527 ± 0.0113	0.2419 ± 0.0008	0.6960 ± 0.0082	$+0.0030 \pm 0.0015$	-0.0034 ± 0.0008
TKG	MRR	0.1173 ± 0.0022	0.0815 ± 0.0029	0.8787 ± 0.0308	$+0.1162 \pm 0.0022$	-0.2245 ± 0.0027

TABLE 8

HotpotQA/RoBERTa candidate-marker control results. All variants use the same candidate-marker input, split, metric, and three seeds. Lower Unsupported@GoldCount is better.

Variant	MRR \uparrow	R@1 \uparrow	Evidence F1 \uparrow	AUPRC \uparrow	Unsupported@GoldCount \downarrow
base	0.9111 ± 0.0045	0.8371 ± 0.0073	0.7751 ± 0.0049	0.8110 ± 0.0065	0.2249 ± 0.0049
param_mlp	0.9036 ± 0.0057	0.8245 ± 0.0106	0.7688 ± 0.0033	0.8103 ± 0.0082	0.2312 ± 0.0033
post_attention_glu	0.9051 ± 0.0039	0.8295 ± 0.0098	0.7629 ± 0.0084	0.8034 ± 0.0116	0.2371 ± 0.0084
attention_readout	0.9125 ± 0.0042	0.8405 ± 0.0072	0.7730 ± 0.0076	0.8129 ± 0.0040	0.2270 ± 0.0076
query_only_gate	0.9078 ± 0.0021	0.8312 ± 0.0048	0.7726 ± 0.0057	0.8104 ± 0.0053	0.2274 ± 0.0057
shuffled_warrant	0.9046 ± 0.0102	0.8270 ± 0.0166	0.7671 ± 0.0160	0.7979 ± 0.0086	0.2329 ± 0.0160
openpath_nogate	0.9129 ± 0.0092	0.8405 ± 0.0165	0.7755 ± 0.0110	0.8102 ± 0.0127	0.2245 ± 0.0110
full_warrant	0.9134 ± 0.0010	0.8414 ± 0.0052	0.7772 ± 0.0058	0.8042 ± 0.0027	0.2228 ± 0.0058

0.2249 to 0.2228, corresponding to an unsupported-attribution error reduction of about 0.94%. Since MRR, R@1, and Evidence F1 also increase, Warrant acts in this setting to reduce unsupported evidence selection.

5.6 Path Localization as a General Adaptation Method

The methodology of Warrant is defined as a path-localization procedure that finds a metric-facing weighted value path. As defined in Section 4.3 and Algorithm 1, the

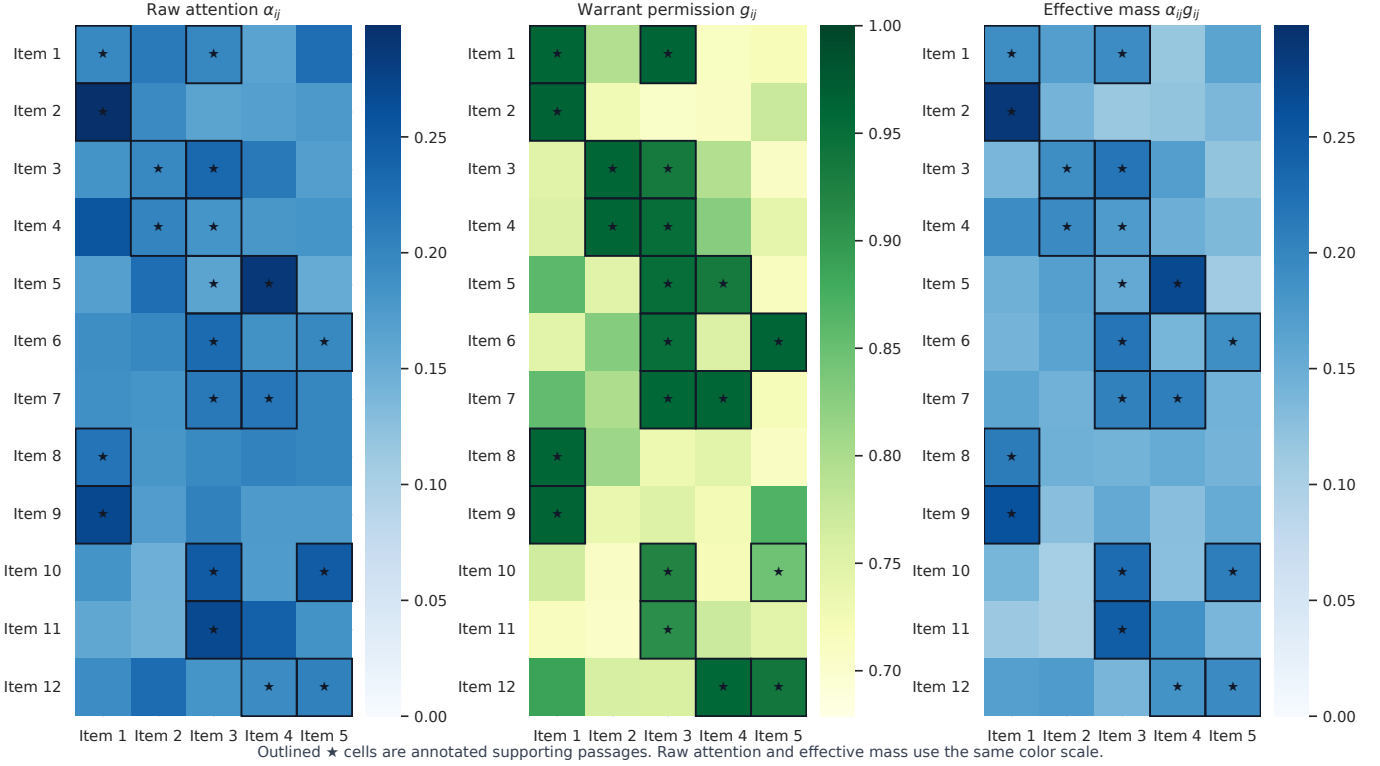


Fig. 5. RAG case study on HotpotQA. The left panel shows raw attention α_{ij} , the middle panel shows Warrant permission g_{ij} , and the right panel shows effective mass $\alpha_{ij}g_{ij}$. Outlines and stars mark annotated supporting-passage cells.

procedure first fixes the prediction object from which the primary metric is computed, then traces whether perturbing a candidate attention-derived weighted value term actually changes that object, and finally places the value-contribution interface at the last item-wise bottleneck. The experiments test whether this tracing protocol applies unchanged across domains. Figure 6 compares the path selected by Algorithm 1 with generic q-k placement and shuffled query-item pairing.

Correct-path Warrant achieves higher direction-aware performance than Base in every domain. In CTDG and TKG, Generic q-k Warrant is nearly flat, whereas Correct-path Warrant yields large improvements. In CTDG, Generic gives only +0.0043 AUC, while Correct-path obtains +0.1119 AUC. In TKG, Generic gives only +0.0004 MRR, while Correct-path obtains +0.0687 MRR. Therefore, performance gains are more closely tied to placement on the metric-defining value path than to the mere presence of a Warrant block.

Shuffled pairing tests the second condition of the method. The improvement depends jointly on the path itself and on the permission relation between the current query and the key-value item. In CTDG, MTPP, and STPP, shuffled pairing is much lower than Correct-path. In RAG and TKG, the shuffled degradation is smaller, but Correct-path still has the highest score. Thus, the general method consists of path localization, which finds the path where the weighted value term reaches the primary metric, and query-item permission, which computes whether the current query authorizes the key-value item’s contribution on that path.

5.7 CTDG Edge-Query Adapter Ablation

In CTDG, the prediction target is the current source-destination edge score rather than a node representation. Therefore, the Warrant query must also represent an edge-level prediction request. The edge-query adapter ablation separates whether this interface can be explained by increased parameters or hand-crafted temporal features. Figure 7 summarizes the ablation results.

Edge-conditioned Warrant obtains an AUC of 0.8980, which is +0.1119 above Base. The parameter control and hand-crafted-only control also provide some improvement, but neither approaches the gain of Edge-conditioned Warrant. When the pairing between the edge query and history item is broken at evaluation time, AUC collapses to 0.6376. This result indicates that the value-contribution interface between the current edge query and source/destination history weighted terms plays a central role in CTDG.

5.8 Explaining Heterogeneity: WNS and Negative-Row Audit

The main benchmark in Section 5.2 shows that the effect of Warrant is not uniform across domains. Improvements are relatively large in CTDG, STPP, and TKG, but small or mixed in MTPP and RAG. Warrant Need Score (WNS) is not a scalar success predictor; it is an operational diagnostic that measures the leverage and localization sensitivity of the metric-facing value path. WNS is computed by directly training and evaluating control variants with the same budget in each representative domain setting; it is not a post hoc

CTDG	✓ +0.112 (3/3)	✓ +0.108 (3/3)	✓ +0.260 (3/3)
MTPP	✓ +0.016 (1/1)	✗ -0.000 (0/1)	✓ +0.017 (1/1)
RAG	✓ +0.002 (1/1)	✓ +0.001 (1/1)	✓ +0.000 (1/1)
STPP	✓ +0.020 (1/1)	✗ -0.007 (0/1)	✓ +0.132 (1/1)
TKG	✓ +0.069 (1/1)	✓ +0.068 (1/1)	✓ +0.003 (1/1)
	Correct > Base	Correct > Generic	Correct > Shuffled

Fig. 6. Path localization check. The figure compares Base, Generic q-k Warrant, Correct-path Warrant, and Shuffled pairing for each domain.

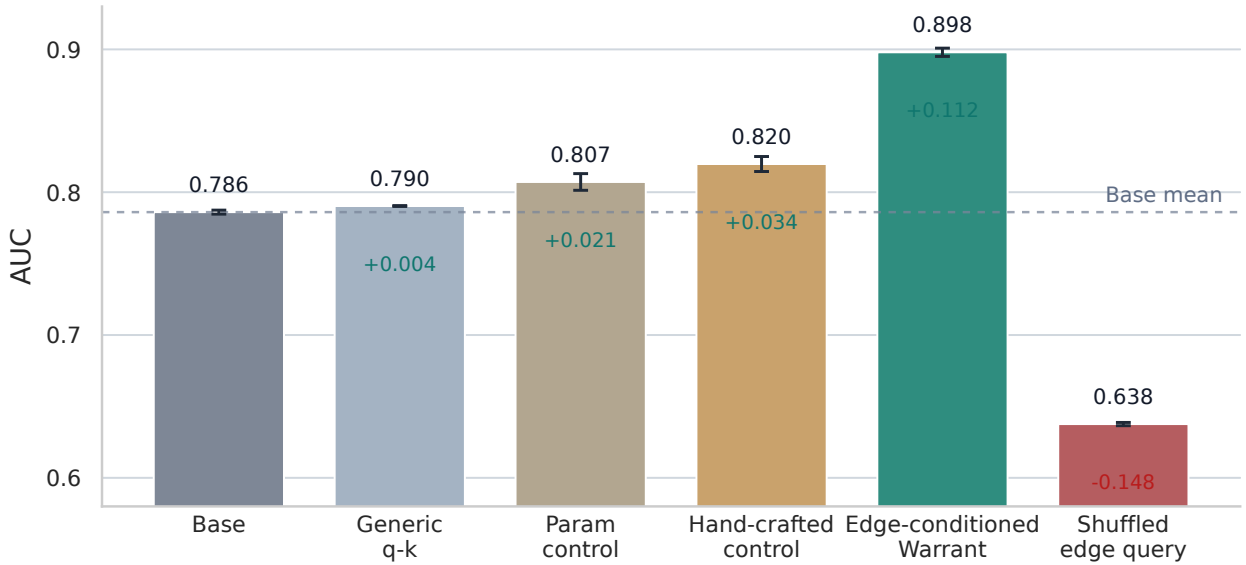


Fig. 7. CTDG edge-query adapter ablation. Edge-conditioned Warrant outperforms generic Warrant, the parameter control, and the hand-crafted control, while a shuffled edge query causes a large performance drop.

combination of the main benchmark, path localization, and mass-diagnostic results in Section 5.2.

For each domain, we compare Base, Generic q-k Warrant, Correct-path Warrant, and Shuffled-pairing Warrant. PathReach asks whether Correct-path Warrant improves over Base; Correct > Generic asks whether metric-facing placement matters; and Correct > Shuffled asks whether query-item pairing matters. Every component is computed as a paired delta with the metric direction taken into account. For higher-is-better metrics, $\Delta(A, B) = A - B$; for lower-is-better metrics, $\Delta(A, B) = B - A$. Raw WNS is a weighted average of the positive parts of the PathReach relative, Correct > Generic relative, and Correct > Shuffled relative components, each divided by the absolute base

metric value. Therefore, a WNS component should be interpreted as a direction-aware delta normalized by the base metric value; it is distinct from an absolute AUC, MRR, or RMSE delta.

Domain-level WNS: Where Does Warrant Have Leverage?

Table 9 reports WNS results together with descriptive correlations to the main-benchmark relative gain from Section 5.2. Because there are only five domains, the correlation p -values should not be interpreted as independent statistical proof; checking the ordering and component pattern is sufficient. WNS and the main-benchmark domain-level relative gain from Section 5.2 show rank consistency, with Pearson $r = 0.765$ and Spearman $\rho = 0.800$. Here, RAG WNS is

a diagnostic for the reference FiD support-passage ranking path, whereas the RoBERTa result in Section 5.5 is a separate evidence-attribution setting that uses candidate sentence marker readout and auxiliary permission supervision.

Domain-level WNS explains why the effect of Warrant is heterogeneous across task families. TKG shows high PathReach and Correct > Generic, indicating a high-leverage historical-tail path. CTDG also shows strong path sensitivity and query-item pairing sensitivity. STPP has strong sensitivity but low PathReach, suggesting that correct query-history pairing matters even though it can interact with continuous dynamics. MTPP and RAG remain at weak or negligible WNS, which is consistent with mixed or tie-level gains.

Negative-row Audit: Sensitivity Without Positive PathReach

Table 10 reports the WNS component audit for the negative rows.

The two negative rows share a PathReach of zero. They therefore do not contradict the domain-level WNS interpretation. Instead, they show cases where the localized path is sensitive or saturated but is not safely improved by a scalar permission interface.

Gowalla / DeepSTPP is not a simple false-suppression case. Under a useful-local-history proxy, Correct-path Warrant preserves target-proximal history more strongly than remaining history. The drop is therefore difficult to explain as suppression of useful local evidence. This row is a case where query-history pairing sensitivity is large without positive PathReach. A more appropriate interpretation is local-prior/dynamics entanglement: Warrant changes the local-history path, but the latent state of DeepSTPP already compresses user-specific revisits, place priors, and mobility dynamics, so a scalar permission perturbation can conflict with short-move or revisit dynamics.

ICEWS18 / CyGNet is better interpreted as a copy-saturated case. PathReach and Correct > Generic are zero, OpenPath-NoGate is almost identical to Base, and the learned copy gate is also close to identity. This suggests that CyGNet already exposes a strong copy path, leaving little room for an additional scalar permission interface to improve performance. In the diagnostic, false-over-true copy imbalance slightly increases after Warrant scaling, which is consistent with copy-calibration risk rather than a missing-path failure.

5.9 Synthesis: Path-Localized Evidence Contributions

The overall experimental flow converges on a single interpretation. The main benchmark in Section 5.2 shows broad positive directionality but also includes mixed and drop rows. Path-exposure and mass diagnostics show that performance depends on the metric-facing contribution path, not on attention relevance itself. Path localization and the CTDG edge-query ablation show that correct placement and query-item pairing matter. Finally, WNS and the negative-row audit explain why the effect of Warrant is heterogeneous across domains and rows. Even when path sensitivity is high, it may not lead to positive reach if the path is entangled with dynamics or already saturated by a prior path.

Therefore, Warrant is best interpreted as a localized interface that exposes and controls weighted value contributions

entering prediction. Edge history in CTDG, event history in MTPP, retrieved passages in RAG, spatio-temporal history in STPP, and historical facts in TKG can all receive attention, but whether their contributions are qualified to enter the metric-facing score or state must be re-decided by the current query and metric path. When this interface is explicitly placed on the value path, relevance is converted into prediction evidence.

6 DISCUSSION, LIMITATION, AND CONCLUSION

Discussion.: The experiments in this paper show that identifying the value path through which attention-formed weighted value terms reach the final metric is the starting point of Warrant adaptation. We first find the path of the weighted value term $\alpha_{ij}v_j$ that flows through attention aggregation into the actual prediction object and determines the primary metric, and then place a path-localized value-contribution interface on that path. When this placement is correct, $\alpha_{ij}v_j$ is replaced by $\alpha_{ij}g_{ij}v_j$, and metric-facing contributions are exposed or controlled more accurately across tasks. The main benchmark, TKG path-exposure ablation, mass diagnostics, HotpotQA/RoBERTa control, path localization, CTDG edge-query ablation, and WNS/negative-row audit all point to the same conclusion. When the interface lies on the metric-defining value path, the weighted value term is exposed as the unit of prediction evidence and, when needed, becomes the target of permission.

In standard attention, α_{ij} simultaneously represents relevance between a query and key and determines the size of the value contribution. Under this structure, once an item is judged relevant, its value term enters the prediction state. Relevance, path exposure, and contribution permission are tied inside a single scalar. Warrant preserves the relevance decision of attention, places the already formed weighted value term on the metric path through which it can affect the current prediction, and, when needed, decides its qualification with a separate gate g_{ij} . The attention output is thereby treated as a path-localized evidence unit.

This decomposition is especially important in domains where the contribution of a relevant key-value item varies with the query and metric path. A retrieved passage can be related to a question without being supporting evidence, a historical fact can be connected to a temporal query without being current true-tail evidence, and temporal history can be related to the current edge while being stale or reinforcing a hard negative. Such items can receive attention, but if their weighted value terms enter the metric-facing path unchanged, they can act as distractors, shortcuts, or stale signals. Evidence is formed when a weighted value term is exposed on the path leading to the primary metric and its contribution is permitted under the current query.

Limitation.: The performance of Warrant is sensitive to how accurately the interface captures the value path of the primary metric. In MTPP, Mark MRR is computed from candidate mark ranking, but the shared state jointly contains mark transitions, temporal intensity, and inter-event time. In data such as Retweets, where the number of marks is small and repeated propagation patterns are strong, past events are more easily used as candidate-specific support. In data

TABLE 9

Dedicated Warrant Need Score (WNS). The upper block summarizes raw WNS, relative WNS, and base-normalized component scores for one representative setting per domain. Component columns are direction-aware differences normalized by the base metric value, not absolute AUC, MRR, or RMSE differences. The lower block reports descriptive correlations with main-benchmark domain-level relative gain; with only five domains, these correlations are used as rank-consistency diagnostics rather than standalone statistical evidence.

Domain-level WNS components								
Domain	Setting	Tier	Summary			Component: direction-aware $\Delta/ Base $		
			WNS	Rel. WNS	Main rel. gain	PathReach rel.	Correct > Generic rel.	Correct > Shuffled rel.
TKG	GDELTA / xERTE	<i>very high</i>	0.5758	1.0000	4.248%	0.9385	0.9351	0.0437
CTDG	LastFM / DyGFormer	<i>strong</i>	0.1322	0.2290	2.896%	0.1143	0.1159	0.1734
STPP	Earthquake / DeepSTPP	<i>strong</i>	0.1157	0.2004	3.557%	0.0074	0.0008	0.3822
MTPP	Retweets / AttNHP	<i>weak</i>	0.0146	0.0247	0.028%	0.0000	0.0000	0.0496
RAG	HotpotQA / FiD	<i>negligible</i>	0.0004	0.0000	0.157%	0.0007	0.0002	0.0000

Descriptive correlation with main-benchmark relative gain				
Predictor	Pearson r	Spearman ρ	Exact p	n
WNS	0.765	0.800	0.133	5
PathReach rel.	0.634	0.900	0.083	5
Correct > Generic rel.	0.630	0.900	0.083	5
Correct > Shuffled rel.	0.522	0.200	0.783	5

TABLE 10

Negative-row WNS component audit. Both rows have zero PathReach, so their WNS reflects sensitivity rather than positive reach over Base.

Negative row	Main Δ	WNS	PathReach	Correct>Generic	Correct>Shuffled
Gowalla / DeepSTPP	-0.42%	12.36	0.000	0.022	37.43
ICEWS18 / CyGNet	-2.24%	0.130	0.000	0.000	0.393

such as StackOverflow, where transitions are more diffuse, the required weak transition signal and shortcut signal can be mixed within the same history term, causing the gate to behave conservatively.

In STPP, the reported metric is Location RMSE, whereas the training objective fits time dynamics and spatial dynamics together. In Earthquake, down-weighting stale spatial history is transmitted relatively stably to the continuous location head. In Gowalla, user-specific check-ins, long-tail place priors, and sparse mobility patterns overlap; when latent dynamics strongly compress history contributions, as in DeepSTPP, residual-path alignment becomes more important. The RAG results are limited to Support MRR for supporting evidence selection and do not directly evaluate answer generation quality. In TKG, historical-tail path exposure can account for a large share of the gain, as in the GDELTA-xERTE diagnostic, and copy-heavy models can show small or negative additional gains because a copy path is already open. These conditions motivate future localization methods that identify metric-facing weighted value paths more finely.

Conclusion.: Relevance is not permission. Attention decides what the model can read, but it does not guarantee that the read value contribution becomes evidence for the current prediction. Warrant finds the weighted value term that is actually transmitted to the primary metric in each task and decides, through path exposure and query-

conditioned permission, whether that term is qualified to enter the prediction under the current query. From this perspective, evidence is a value contribution permitted on the metric path, and it is distinct from attention mass. A weighted value term becomes evidence only when it is warranted on the path to the metric.

DECLARATION OF COMPETING INTEREST

The authors declare that they have no known competing financial interests or personal relationships that could have appeared to influence the work reported in this paper.

ACKNOWLEDGEMENTS

The authors have no acknowledgements to declare.

DATA AVAILABILITY

All datasets used in this study are publicly available. The exact data sources are listed in Table 11.

CODE AVAILABILITY

The implementation, experiment configurations, aggregation scripts, and plotting scripts used in this study are available at <https://github.com/SnowyPainter/warrant-public>.

TABLE 11
Public dataset sources used in this study.

Domain	Dataset	Source
CTDG	Wikipedia	https://snap.stanford.edu/jodie/wikipedia.csv
CTDG	MOOC	https://snap.stanford.edu/jodie/mooc.csv
CTDG	LastFM	https://snap.stanford.edu/jodie/lastfm.csv
MTPP	StackOverflow	HuggingFace: https://huggingface.co/datasets/easytpp/stackoverflow
MTPP	Retweets	HuggingFace: https://huggingface.co/datasets/easytpp/retweet
STPP	Earthquake	GitHub: https://github.com/ss15859/EarthquakeNPP
STPP	Gowalla	https://snap.stanford.edu/data/loc-gowalla_totalCheckins.txt.gz
TKG	ICEWS14	GitHub RE-Net data: https://github.com/INK-USC/RE-Net
TKG	ICEWS18	GitHub RE-Net data: https://github.com/INK-USC/RE-Net
TKG	GDELT	GitHub RE-Net data: https://github.com/INK-USC/RE-Net
RAG	HotpotQA	HuggingFace: https://huggingface.co/datasets/hotpotqa/hotpot_qa

REFERENCES

- [1] A. Vaswani, N. Shazeer, N. Parmar, J. Uszkoreit, L. Jones, A. N. Gomez, L. Kaiser, and I. Polosukhin, "Attention is all you need," in *Advances in Neural Information Processing Systems*, 2017. [Online]. Available: <https://papers.nips.cc/paper/7181-attention-is-all-you-need>
- [2] D. Xu, C. Ruan, E. Körpeoğlu, S. Kumar, and K. Achan, "Inductive representation learning on temporal graphs," in *International Conference on Learning Representations*, 2020. [Online]. Available: <https://openreview.net/forum?id=rjEW1yHYwH>
- [3] L. Yu, L. Sun, B. Du, and W. Lv, "Towards better dynamic graph learning: New architecture and unified library," in *Advances in Neural Information Processing Systems*, 2023. [Online]. Available: https://proceedings.neurips.cc/paper_files/paper/2023/hash/d611019afba70d547bd595e8a4158f55-Abstract-Conference.html
- [4] P. Lewis, E. Perez, A. Piktus, F. Petroni, V. Karpukhin, N. Goyal, H. Küttler, M. Lewis, W.-t. Yih, T. Rocktäschel, S. Riedel, and D. Kiela, "Retrieval-augmented generation for knowledge-intensive nlp tasks," in *Advances in Neural Information Processing Systems*, 2020. [Online]. Available: <https://proceedings.neurips.cc/paper/2020/hash/6b493230205f780e1bc26945df7481e5-Abstract.html>
- [5] R. K. Srivastava, K. Greff, and J. Schmidhuber, "Highway networks," in *ICML Deep Learning Workshop*, 2015. [Online]. Available: <https://arxiv.org/abs/1505.00387>
- [6] S. Hochreiter and J. Schmidhuber, "Long short-term memory," *Neural Computation*, vol. 9, no. 8, pp. 1735–1780, 1997.
- [7] K. Cho, B. van Merriënboer, C. Gulcehre, D. Bahdanau, F. Bougares, H. Schwenk, and Y. Bengio, "Learning phrase representations using rnn encoder-decoder for statistical machine translation," *arXiv preprint arXiv:1406.1078*, 2014. [Online]. Available: <https://arxiv.org/abs/1406.1078>
- [8] E. Perez, F. Strub, H. de Vries, V. Dumoulin, and A. Courville, "Film: Visual reasoning with a general conditioning layer," in *Proceedings of the AAAI Conference on Artificial Intelligence*, 2018. [Online]. Available: <https://arxiv.org/abs/1709.07871>
- [9] N. Shazeer, A. Mirhoseini, K. Maziarz, A. Davis, Q. Le, G. Hinton, and J. Dean, "Outrageously large neural networks: The sparsely-gated mixture-of-experts layer," in *International Conference on Learning Representations*, 2017. [Online]. Available: <https://openreview.net/forum?id=B1ckMDqlg>
- [10] D. Bahdanau, K. Cho, and Y. Bengio, "Neural machine translation by jointly learning to align and translate," in *International Conference on Learning Representations*, 2015. [Online]. Available: <https://arxiv.org/abs/1409.0473>
- [11] S. Sukhbaatar, J. Weston, R. Fergus *et al.*, "End-to-end memory networks," in *Advances in Neural Information Processing Systems*, 2015. [Online]. Available: <https://papers.nips.cc/paper/5846-end-to-end-memory-networks>
- [12] Y. N. Dauphin, A. Fan, M. Auli, and D. Grangier, "Language modeling with gated convolutional networks," in *Proceedings of the 34th International Conference on Machine Learning*, 2017, pp. 933–941.
- [13] J. Hu, L. Shen, and G. Sun, "Squeeze-and-excitation networks," in *Proceedings of the IEEE Conference on Computer Vision and Pattern Recognition*, 2018, pp. 7132–7141.
- [14] B. Dhingra, H. Liu, Z. Yang, W. W. Cohen, and R. Salakhutdinov, "Gated-attention readers for text comprehension," in *Proceedings of the 55th Annual Meeting of the Association for Computational Linguistics*, 2017, pp. 1832–1846. [Online]. Available: <https://aclanthology.org/P17-1168/>
- [15] E. Parisotto, H. F. Song, J. W. Rae, R. Pascanu, C. Gulcehre, S. M. Jayakumar, M. Jaderberg, R. L. Kaufman, A. Clark, S. Noury, M. Botvinick, N. Heess, and R. Hadsell, "Stabilizing transformers for reinforcement learning," *Proceedings of the 37th International Conference on Machine Learning*, 2020. [Online]. Available: <https://proceedings.mlr.press/v119/parisotto20a.html>
- [16] X. Ma, C. Zhou, X. Kong, J. He, L. Gui, G. Neubig, J. May, and L. Zettlemoyer, "Mega: Moving average equipped gated attention," in *International Conference on Learning Representations*, 2023.
- [17] K. Xu, J. Ba, R. Kiros, K. Cho, A. Courville, R. Salakhutdinov, R. Zemel, and Y. Bengio, "Show, attend and tell: Neural image caption generation with visual attention," in *Proceedings of the 32nd International Conference on Machine Learning*, 2015, pp. 2048–2057.
- [18] A. F. T. Martins and R. F. Astudillo, "From softmax to sparsemax: A sparse model of attention and multi-label classification," in *Proceedings of the 33rd International Conference on Machine Learning*, 2016, pp. 1614–1623.
- [19] A. See, P. J. Liu, and C. D. Manning, "Get to the point: Summarization with pointer-generator networks," in *Proceedings of the 55th Annual Meeting of the Association for Computational Linguistics*, 2017, pp. 1073–1083.
- [20] V. Karpukhin, B. Oguz, S. Min, P. Lewis, L. Wu, S. Edunov, D. Chen, and W.-t. Yih, "Dense passage retrieval for open-domain question answering," in *Proceedings of the 2020 Conference on Empirical Methods in Natural Language Processing*, 2020, pp. 6769–6781. [Online]. Available: <https://aclanthology.org/2020.emnlp-main.550/>
- [21] G. Izacard and E. Grave, "Leveraging passage retrieval with generative models for open domain question answering," in *Proceedings of the 16th Conference of the European Chapter of the Association for Computational Linguistics*, 2021, pp. 874–880. [Online]. Available: <https://aclanthology.org/2021.eacl-main.74/>
- [22] I. Beltagy, M. E. Peters, and A. Cohan, "Longformer: The long-document transformer," *arXiv preprint arXiv:2004.05150*, 2020. [Online]. Available: <https://arxiv.org/abs/2004.05150>
- [23] R. Nogueira and K. Cho, "Passage re-ranking with bert," *arXiv preprint arXiv:1901.04085*, 2019. [Online]. Available: <https://arxiv.org/abs/1901.04085>
- [24] C. Guo, G. Pleiss, Y. Sun, and K. Q. Weinberger, "On calibration of modern neural networks," in *Proceedings of the 34th International Conference on Machine Learning*, 2017, pp. 1321–1330. [Online]. Available: <https://proceedings.mlr.press/v70/guo17a.html>
- [25] Y. Geifman and R. El-Yaniv, "Selective classification for deep neural networks," in *Advances in Neural Information Processing Systems*, 2017. [Online]. Available: <https://papers.nips.cc/paper/7073-selective-classification-for-deep-neural-networks>

[26] Y. Liu, M. Ott, N. Goyal, J. Du, M. Joshi, D. Chen, O. Levy, M. Lewis, L. Zettlemoyer, and V. Stoyanov, "Roberta: A robustly optimized bert pretraining approach," *arXiv preprint arXiv:1907.11692*, 2019. [Online]. Available: <https://arxiv.org/abs/1907.11692>

APPENDIX A THEORETICAL DERIVATIONS

This appendix summarizes the mathematical structure by which Warrant operates as a permission operator on metric-facing attention-weighted value terms. For a single query, write

$$h = \sum_j \alpha_j v_j, \quad c_j = \alpha_j v_j,$$

$$h^W = \sum_j \alpha_j g_j v_j = \sum_j g_j c_j, \quad g_j = \lambda + (1 - \lambda)\sigma(\psi_j).$$

Here, $\lambda > 0$ is the leak factor. Thus, Warrant is not a hard mask, and every valid item retains a minimal value/gradient path.

A.1 Gate Gradient

Let the metric-facing loss be $\mathcal{L}(h^W)$. Since ψ_j directly affects only g_j ,

$$\frac{\partial h^W}{\partial g_j} = \alpha_j v_j = c_j,$$

$$\frac{\partial g_j}{\partial \psi_j} = (1 - \lambda)\sigma'(\psi_j),$$

$$\frac{\partial \mathcal{L}}{\partial \psi_j} = (1 - \lambda)\sigma'(\psi_j) \langle \nabla_{h^W} \mathcal{L}, c_j \rangle.$$

By the chain rule, the gate receives an item-wise loss-aligned signal for the weighted value term itself. If the inner product is positive, the contribution points in a loss-increasing direction, and gradient descent lowers the permission logit. If the inner product is negative, the contribution points in a loss-reducing direction, and the gate moves toward preservation.

A.2 Local Loss Bound

Assume that \mathcal{L} is β -smooth with respect to the prediction representation. Taking the base state as $h = \sum_j c_j$ and scaling only item j ,

$$h(g_j) = h + (g_j - 1)c_j.$$

The smoothness condition gives the following bound.

$$\mathcal{L}(h(g_j)) \leq \mathcal{L}(h) + (g_j - 1) \langle \nabla \mathcal{L}(h), c_j \rangle + \frac{\beta}{2}(g_j - 1)^2 \|c_j\|^2,$$

$$\gamma_j = \langle \nabla \mathcal{L}(h), c_j \rangle,$$

$$g_j^* = \Pi_{[\lambda, 1]} \left(1 - \frac{\gamma_j}{\beta \|c_j\|^2} \right).$$

Up to constants, this is a one-dimensional quadratic. Therefore, a harmful contribution with positive gradient alignment is reduced, whereas a helpful contribution with negative alignment is preserved at $g_j = 1$ by projection.

A.3 Manifold-Local Permission Rule

The Euclidean local rule in the main text is written in the ambient representation space. Suppose that the prediction state lies near a local C^2 representation manifold $\mathcal{M} \subset \mathbb{R}^d$, with tangent space $T_h \mathcal{M}$ and tangent projection P_h . Writing $g_j = 1 - \delta_j$, the Warrant perturbation is

$$\Delta(g) = \sum_j (g_j - 1)c_j = - \sum_j \delta_j c_j$$

and the component that directly enters first-order loss change on the manifold is

$$\xi(g) = P_h \Delta(g) = - \sum_j \delta_j P_h c_j.$$

Let $\tilde{c}_j = P_h c_j$. Riemannian smoothness with respect to a local retraction R_h gives

$$\mathcal{L}(R_h(\xi)) \leq \mathcal{L}(h) + \langle \text{grad}_{\mathcal{M}} \mathcal{L}(h), \xi \rangle + \frac{\beta_{\mathcal{M}}}{2} \|\xi\|^2.$$

If only a single contribution is controlled, then $\xi = -\delta_j \tilde{c}_j$, and the upper bound excluding constants is

$$-\delta_j \langle \text{grad}_{\mathcal{M}} \mathcal{L}(h), \tilde{c}_j \rangle + \frac{\beta_{\mathcal{M}}}{2} \delta_j^2 \|\tilde{c}_j\|^2.$$

Thus, when $\epsilon = 0$, the unconstrained minimizer is

$$\delta_j = \frac{\langle \text{grad}_{\mathcal{M}} \mathcal{L}(h), \tilde{c}_j \rangle}{\beta_{\mathcal{M}} \|\tilde{c}_j\|^2}.$$

Projecting this value to the feasible interval $[0, 1 - \lambda]$ yields the rule in the main text. The ϵ in the main-text expression is a numerical stabilizer used when $\|\tilde{c}_j\|$ is close to zero; it is not part of the exact minimizer itself. This result is a local tangent-space descent interpretation, not a global optimality statement.

A.4 Tangent Gram Matrix and Entangled Paths

When multiple contributions are controlled simultaneously, $\xi(g) = - \sum_j \delta_j \tilde{c}_j$. Define

$$a_j = \langle \text{grad}_{\mathcal{M}} \mathcal{L}(h), \tilde{c}_j \rangle, \quad G_{jk} = \langle \tilde{c}_j, \tilde{c}_k \rangle.$$

Substituting into the Riemannian smoothness bound gives

$$\mathcal{L}(R_h(\xi(g))) \leq \mathcal{L}(h) - \sum_j \delta_j a_j + \frac{\beta_{\mathcal{M}}}{2} \left\| \sum_j \delta_j \tilde{c}_j \right\|^2$$

$$= \mathcal{L}(h) - \delta^\top a + \frac{\beta_{\mathcal{M}}}{2} \delta^\top G \delta.$$

Here, G is the Gram matrix of tangent contributions. It is not precise to always call off-diagonal entries penalties. Since G_{jk} can be negative, they are more safely interpreted as off-diagonal tangent coupling or cross terms. However, large positive off-diagonal coupling, or large-magnitude off-diagonal coupling, can destabilize diagonal item-wise shrinkage. In this case, useful contributions and shortcut/noisy contributions share the same local tangent subspace, so scalar item-wise permission can become conservative or miscalibrated.

A.5 Smooth Bounded Parameterization and Stationary Scope

The leak-sigmoid gate is defined as

$$g_j = \lambda + (1 - \lambda)\sigma(\psi_j),$$

so

$$g_j \in [\lambda, 1], \quad \left| \frac{\partial g_j}{\partial \psi_j} \right| = (1 - \lambda)\sigma(\psi_j)(1 - \sigma(\psi_j)) \leq \frac{1 - \lambda}{4}.$$

Also, because $\delta_j = 1 - g_j \in [0, 1 - \lambda]$,

$$\|\Delta(g)\| = \left\| \sum_j (g_j - 1)c_j \right\| \leq \sum_j \delta_j \|c_j\| \leq (1 - \lambda) \sum_j \|c_j\|.$$

Therefore, Warrant is not a hard discontinuous mask but a smooth bounded perturbation of the base value path. Under standard smooth nonconvex SGD assumptions that the base network and ψ_j network are smooth and stochastic gradients are unbiased with bounded variance, the augmented objective $F(\theta)$ also has a finite smoothness constant. For step size $\eta \leq 1/L_F$, the standard descent lemma gives a convergence-to-stationarity bound of the form

$$\frac{1}{T} \sum_{t=0}^{T-1} \mathbb{E} \|\nabla F(\theta_t)\|^2 \leq \frac{2(F(\theta_0) - F_*)}{\eta T} + L_F \eta \sigma_g^2.$$

This is not a guarantee of global convergence specific to Warrant or of performance improvement over the base model. It is a scope statement that the bounded smooth parameterization does not break ordinary smooth trainability.

A.6 SNR Condition

Decompose the metric-facing contribution into support signal and noisy non-support terms.

$$h_B = \sum_{j \in S} \alpha_j \mu_j + \sum_{j \in N} \alpha_j \xi_j, \quad \mathbb{E}[\xi_j] = 0, \quad \text{Var}(\xi_j) = \sigma_j^2,$$

$$\text{SNR}_B = \frac{\sum_{j \in S} \alpha_j \mu_j}{\sqrt{\sum_{j \in N} \alpha_j^2 \sigma_j^2}},$$

$$\text{SNR}_W = \frac{\sum_{j \in S} \alpha_j g_j \mu_j}{\sqrt{\sum_{j \in N} \alpha_j^2 g_j^2 \sigma_j^2}}.$$

The SNRs of Base and Warrant are SNR_B and SNR_W , respectively. Support signal retention and noise standard-deviation retention are

$$R_S = \frac{\sum_{j \in S} \alpha_j g_j \mu_j}{\sum_{j \in S} \alpha_j \mu_j},$$

$$R_N = \sqrt{\frac{\sum_{j \in N} \alpha_j^2 g_j^2 \sigma_j^2}{\sum_{j \in N} \alpha_j^2 \sigma_j^2}},$$

$$\frac{\text{SNR}_W}{\text{SNR}_B} = \frac{R_S}{R_N},$$

$$\text{SNR}_W > \text{SNR}_B \iff R_S > R_N.$$

This condition does not require perfect preservation of the support signal. SNR increases when the support signal is retained more strongly than the noise standard deviation.

A.7 High-Probability Interpretation

The values appearing in the SNR condition are computed as weighted averages. Define the weights

$$w_j^S = \frac{\alpha_j \mu_j}{\sum_{l \in S} \alpha_l \mu_l},$$

$$w_j^N = \frac{\alpha_j^2 \sigma_j^2}{\sum_{l \in N} \alpha_l^2 \sigma_l^2},$$

$$R_S = \sum_{j \in S} w_j^S g_j, \quad R_N = \sum_{j \in N} w_j^N g_j^2.$$

Because $g_j \in [\lambda, 1]$, both quantities are bounded weighted averages. If evidence-aligned permission creates a positive expectation margin between the weighted support gate and the weighted noisy gate RMS, concentration of bounded weighted averages makes the probability of the false-suppression event $R_S \leq R_N$ decrease as the effective number of support/noise items grows. Thus, the alignment margin controls the probability of SNR degradation.

A.8 Gradient Noise and Effective Curvature

Let ξ_j be a noisy value-gradient component. The base path transmits $\alpha_j \xi_j$, whereas the Warrant path transmits $\alpha_j g_j \xi_j$. Therefore,

$$\text{Var}[\alpha_j g_j \xi_j] = \alpha_j^2 g_j^2 \text{Var}[\xi_j] \leq \alpha_j^2 \text{Var}[\xi_j],$$

$$\|\nabla_{v_j}^2 \mathcal{L}\|_{\text{base}} \leq \alpha_j^2 \beta,$$

$$\|\nabla_{v_j}^2 \mathcal{L}\|_{\text{warrant}} \leq \alpha_j^2 g_j^2 \beta \leq \alpha_j^2 \beta.$$

Likewise, if \mathcal{L} is β -smooth with respect to h , the second line holds along the item value direction v_j . This bound is path-local. A down-weighted metric-facing value path reduces gradient-noise and effective-curvature exposure on that path.

A.9 Diagonal Permission vs. Softmax Reweighting

Let $m_j^W = \alpha_j g_j$. Since Warrant does not recompute the attention softmax,

$$\frac{\partial m_j^W}{\partial \psi_l} = \alpha_j (1 - \lambda) \sigma'(\psi_j) \mathbf{1}[j = l],$$

$$\tilde{\alpha}_j = \text{softmax}_j(s_j + \log g_j),$$

$$\frac{\partial \tilde{\alpha}_j}{\partial \log g_l} = \tilde{\alpha}_j (\mathbf{1}[j = l] - \tilde{\alpha}_l).$$

The first derivative has an item-wise diagonal structure. In contrast, attention-logit gating couples all items through softmax normalization. Therefore, Warrant scales contributions while preserving relevance α_j , whereas logit gating changes the relevance distribution itself.

A.10 Post-Attention Gates and Path Localization

A post-attention gate $F(h)$ sees only the aggregate $h = \sum_j \alpha_j v_j$. If different item decompositions produce the same h , then $F(h)$ cannot assign different permissions to the underlying items. For example, if $v_1 = u$, $v_2 = -u$, and $\alpha_1 = \alpha_2 = 0.5$, then the aggregate is $h = 0$. A post-attention gate sees only $h = 0$, so it cannot permit v_1 and v_2 differently, whereas Warrant can express $g_1 \neq g_2$ in $h^W = 0.5g_1u + 0.5g_2(-u)$.

An attention-logit gate can preserve item identity, but softmax normalization redistributes attention mass. Lowering one item automatically increases the mass of other items. Warrant instead uses $m_j^W = \alpha_j g_j$ and does not enforce $\sum_j m_j^W = 1$. This operation corresponds to attenuation of weighted value contributions rather than redistribution of relevance.

Table 12 summarizes the same-aggregate constructive check.

In contrast, Warrant is applied before item identity disappears.

$$h^W = \sum_j \alpha_j g(q, k_j) v_j,$$

$$\frac{\partial \mathcal{L}}{\partial \psi_j} = (1 - \lambda) \sigma'(\psi_j) \left\langle J_p^\top \nabla_z \mathcal{L}, \alpha_j v_j \right\rangle, \quad J_p = \frac{\partial z}{\partial h_p}.$$

Here, the gated path is $h_p = \sum_j \alpha_j g_j v_j$, and the metric object is $z = f(h_p)$. The gate learning signal is proportional to the path-to-metric Jacobian. This is the mathematical reason for path localization. If Warrant is placed on a path weakly connected to the metric, the permission signal is also weak; correct-path placement exposes the weighted value term that actually changes the reported metric.

APPENDIX B MONTE CARLO DETAILS

Figure 3 visualizes the SNR condition derived in Appendix A.6. The left panel shows the deterministic boundary $R_S = R_N$, where R_S and R_N are the support-signal retention and noise-standard-deviation retention defined in Appendix A.6. The right panel samples the same quantities under an evidence-aligned gate regime. The weighted-average interpretation follows Appendix A.7.

For each trial, we sample a support item set S and a noisy item set N . The simulation uses $|S| = 8$ support items and $|N| = 32$ noisy items. Attention weights for support and noisy items are independently sampled from normalized Gamma variables to form random simplex weights. Support signal magnitudes μ_j and noise standard deviations σ_j are sampled from log-normal distributions to avoid a degenerate equal-weight setting.

$$\mu_j \sim \text{LogNormal}(0, 0.25^2), \quad \sigma_j \sim \text{LogNormal}(0, 0.25^2).$$

Gate variables are sampled from Beta distributions. In the evidence-aligned regime of Figure 3, the support gate mean is set to 0.72, the noisy gate mean to 0.60, and both distributions use concentration parameter 30.

$$g_j^S \sim \text{Beta}(0.72 \cdot 30, (1 - 0.72) \cdot 30),$$

$$g_j^N \sim \text{Beta}(0.60 \cdot 30, (1 - 0.60) \cdot 30).$$

This is a weak alignment setting rather than a near-perfect separator. Support gates are only moderately larger than noisy gates, and some sampled points remain in the degradation region.

For each trial, R_S , R_N , and $\text{SNR}_W/\text{SNR}_B = R_S/R_N$ are computed according to the definitions in Appendix A.6. A trial is counted as improved when $R_S > R_N$. The number of trials is 2,500, with a fixed random seed. Under this weak evidence-aligned regime, 98.2% of sampled operating

points lie in the $R_S > R_N$ region, and the median SNR ratio is $1.19\times$. If the support gate becomes lower than the noisy gate, sampled points move toward the degradation region described in Appendix D.

APPENDIX C MANIFOLD-LOCAL SIMULATION

This appendix provides a synthetic bound decomposition that illustrates the tangent Gram bound in Appendix A.4. It is an illustrative instantiation showing how the cross term $\delta^\top G \delta$ can reduce the benefit of diagonal shrinkage. With two tangent contributions, set $a = (1, 1)$, $\delta = (0.5, 0.5)$, and

$$G = \begin{bmatrix} 1 & \rho \\ \rho & 1 \end{bmatrix}.$$

Then the descent term is $\delta^\top a = 1.0$, and the bound change is

$$\Delta_{\text{bound}} = -\delta^\top a + \frac{\beta_{\mathcal{M}}}{2} \delta^\top G \delta.$$

Table 13 shows that the cross term grows as ρ and curvature $\beta_{\mathcal{M}}$ increase, and that the bound can become positive in a high-curvature entangled case.

This simulation aligns with the negative-row interpretation in Section 5.8. Even when path sensitivity is high, scalar item-wise permission may not lead to safe positive reach if useful contributions and shortcut/noisy contributions are strongly entangled in the tangent space.

APPENDIX D FAILURE REGIMES

The same analysis identifies three failure regimes. First, *false suppression* occurs when support items receive low gates and $R_S \leq R_N$. Second, *unaligned permission* occurs when noisy or shortcut items receive gates as high as support items, so noise retention does not decrease. Third, *weak path localization* occurs when Warrant is placed on a path with a small path-to-metric Jacobian, causing gates to receive only weak metric-facing learning signals. Therefore, the experiments jointly evaluate diagnostics such as the primary metric, support/distractor mass, gate ratios, and correct-path versus generic placement.

APPENDIX E ADDITIONAL HOTPOTQA/ROBERTA DETAILS

This appendix provides detailed settings, full per-variant results, and permission diagnostics for the pretrained RoBERTa supporting sentence selection control in Section 5.5. The main text presents one control table and the core interpretation, while the appendix supplements it with input construction, training settings, readout variants, and seed-wise mean/std results.

Table 14 describes the candidate-marker control setting, Table 15 reports full per-variant results, and Table 16 reports the permission diagnostics.

TABLE 12

Same-aggregate constructive check. This toy check is a constructive experiment that isolates function-class differences between gated objects.

Variant	Item identity available	Attention renormalized	Expected accuracy	Interpretation
post_attention_gate	no	no	0.5	aggregate gate sees the same zero vector for both labels
attention_logit_gate	yes	yes	1.0	separates items by redefining attention mass
warrant_value_term_gate	yes	no	1.0	keeps α fixed and changes item-wise weighted value contribution

TABLE 13

Synthetic manifold-local bound decomposition. The table is an illustrative instantiation of Appendix A.4, not a benchmark result. Larger off-diagonal tangent coupling increases the cross term and can overturn the diagonal shrinkage benefit under high curvature.

Regime	$\beta_{\mathcal{M}}$	ρ	$-\delta^{\top} a$	diagonal term	cross term	Δ_{bound}
Low entanglement	1.0	0.05	-1.000	0.250	0.013	-0.738
Moderate entanglement	1.0	0.40	-1.000	0.250	0.100	-0.650
High entanglement	1.0	0.80	-1.000	0.250	0.200	-0.550
High-curvature entangled	3.0	0.80	-1.000	0.750	0.600	+0.350

TABLE 14

HotpotQA/RobERTa candidate-marker control setting. This experiment does not evaluate answer generation; it is an encoder-side evidence-attribution task that ranks whether a candidate sentence is annotated supporting evidence.

Group	Component	Setting
Encoder	base model	roberta-base
Data	dataset	HotpotQA processed supporting sentence candidates
Input	format	question + instruction + $\langle C0 \rangle, \dots, \langle C7 \rangle$ candidate evidence sentences
Input	candidate count	maximum 8 candidates per question
Input	candidate composition	supporting candidates + hard distractors + random distractors
Training	questions / seeds / epochs	maximum 2,000 questions; seeds 7, 17, 37; 2 epochs
Training	main loss	candidate-wise binary cross entropy
Training	permission auxiliary	weak pairwise gate-alignment auxiliary loss
Evaluation	primary metric	Support MRR over candidate ranking
Evaluation	unsupported attribution	unsupported candidate selected within gold-count budget
Control	base	final candidate marker readout baseline
Control	param_mlp	parameter-count control without value-term permission
Control	post_attention_glu	aggregate/readout gate after item identity is mixed
Control	attention_readout	ungated candidate-marker value-path exposure
Control	query_only_gate	generic permission without item key conditioning
Control	shuffled_warrant	query-item pairing is broken
Control	openpath_nogate	same metric-facing path with $g = 1$
Control	full_warrant	$\alpha_{ij} v_j \mapsto \alpha_{ij} g_{ij} v_j$ on the candidate-marker value path

TABLE 15

HotpotQA/RobERTa supporting sentence selection full control results. Values are means and standard deviations over three seeds. Bold indicates the best value for each metric.

Variant	MRR \uparrow	R@1 \uparrow	Evidence F1 \uparrow	AUPRC \uparrow	Unsupported@GoldCount \downarrow
base	0.9111 \pm 0.0045	0.8371 \pm 0.0073	0.7751 \pm 0.0049	0.8110 \pm 0.0065	0.2249 \pm 0.0049
param_mlp	0.9036 \pm 0.0057	0.8245 \pm 0.0106	0.7688 \pm 0.0033	0.8103 \pm 0.0082	0.2312 \pm 0.0033
post_attention_glu	0.9051 \pm 0.0039	0.8295 \pm 0.0098	0.7629 \pm 0.0084	0.8034 \pm 0.0116	0.2371 \pm 0.0084
attention_readout	0.9125 \pm 0.0042	0.8405 \pm 0.0072	0.7730 \pm 0.0076	0.8129 \pm 0.0040	0.2270 \pm 0.0076
query_only_gate	0.9078 \pm 0.0021	0.8312 \pm 0.0048	0.7726 \pm 0.0057	0.8104 \pm 0.0053	0.2274 \pm 0.0057
shuffled_warrant	0.9046 \pm 0.0102	0.8270 \pm 0.0166	0.7671 \pm 0.0160	0.7979 \pm 0.0086	0.2329 \pm 0.0160
openpath_nogate	0.9129 \pm 0.0092	0.8405 \pm 0.0165	0.7755 \pm 0.0110	0.8102 \pm 0.0127	0.2245 \pm 0.0110
full_warrant	0.9134 \pm 0.0010	0.8414 \pm 0.0052	0.7772 \pm 0.0058	0.8042 \pm 0.0027	0.2228 \pm 0.0058

TABLE 16

HotpotQA/RoBERTa permission diagnostic. The Gold/Random ratio is the average mass ratio between annotated supporting candidates and random distractors.

Variant	Gate mean	Gold gate	Random gate	Gold/Random α	Gold/Random αg
attention_readout	0.3671	0.8688	0.1745	0.3811	2.2536
query_only_gate	0.5416	0.8610	0.4161	0.9987	5.0091
shuffled_warrant	0.9994	0.9994	0.9994	0.9013	0.9015
openpath_nogate	1.0000	1.0000	1.0000	0.6265	0.6265
full_warrant	0.5319	0.8647	0.4049	0.8179	3.8522